UNIVERSIDADE FEDERAL DO CEARÁ

CENTRO DE TECNOLOGIA

DEPARTAMENTO DE ENGENHARIA QUÍMICA

PROGRAMA DE PÓS-GRADUAÇÃO EM ENGENHARIA QUÍMICA

FERNANDA SILVA MOREIRA

CO_2 ADSORPTION ON 13X BINDER FREE ZEOLITE: EFFECT OF SO_2 ADSORPTION ON CO_2 CAPTURE

FORTALEZA

2024

FERNANDA SILVA MOREIRA

CO$_2$ ADSORPTION ON 13X BINDER FREE ZEOLITE: EFFECT OF SO$_2$ ADSORPTION ON CO$_2$ CAPTURE

Dissertação apresentada ao Programa de Pós-Graduação em Engenharia Química da Universidade Federal do Ceará, como requisito parcial à obtenção do título de Mestre em Engenharia Química. Área de concentração: Processos Químicos e Bioquímicos.

Orientador: Prof. Dr. Enrique Vilarrasa Garcia
Coorientadores: Profa. Dra. Diana Cristina Silva de Azevedo e Prof. Dr. Moisés Bastos Neto

FORTALEZA

2024

FERNANDA SILVA MOREIRA

CO$_2$ ADSORPTION ON 13X BINDER FREE ZEOLITE: EFFECT OF SO$_2$ ADSORPTION ON CO$_2$ CAPTURE

Dissertação apresentada ao Programa de Pós-Graduação em Engenharia Química da Universidade Federal do Ceará, como requisito parcial à obtenção do título de Mestre em Engenharia Química. Área de concentração: Processos Químicos e Bioquímicos.

Orientador: Prof. Dr. Enrique Vilarrasa Garcia
Coorientadores: Profa. Dra. Diana Cristina Silva de Azevedo e Prof. Dr. Moisés Bastos Neto.

Aprovada em: 19/02/2024.

BANCA EXAMINADORA

Documento assinado digitalmente
ENRIQUE VILARRASA GARCIA
Data: 20/02/2024 11:45:03-0300
Verifique em https://validar.iti.gov.br

_____

Prof. Dr. Enrique Vilarrasa Garcia (Orientador)
Universidade Federal do Ceará (UFC)

Documento assinado digitalmente
RAFAELLE GOMES SANTIAGO
Data: 20/02/2024 08:26:00-0300
Verifique em https://validar.iti.gov.br

_____

Profa. Dra. Rafaelle Gomes Santiago
Universidade Federal do Ceará (UFC)

Documento assinado digitalmente
MARCELO MARTINS SECKLER
Data: 19/02/2024 19:19:59-0300
Verifique em https://validar.iti.gov.br

_____

Prof. Dr. Marcelo Martins Seckler
Universidade de São Paulo (USP)

"Nobody said it was easy

No one ever said
It would be this hard"

Coldplay - *The Scientist*

AGRADECIMENTOS

Dedico a presente pesquisa aos meus avós maternos, Antônio Ribeiro Silva e Raimunda Edisse Silveira Silva, que mesmo sem nunca terem tido a oportunidade de estudar, sempre valorizaram o esforço de todos os netos em perseguir os estudos. Por isso, e por todo o carinho que tive deles durante a infância, dedico este trabalho a eles.

Agradeço, ainda, a minha irmã, Juliana Moreira, por estar ao meu lado em toda essa jornada. Pelas caronas ao longo dos anos, por ser alguém que eu sempre pude discutir sobre meus trabalhos, reclamar sobre a pesquisa e por sempre estar lá quando eu precisasse, não importando o motivo.

Ao Iveltyma Roosemalen, meu esposo, por todas as piadinhas quando eu mais precisei descontrair e por sempre escutar quando eu ficava nervosa por algum motivo, agradeço por estar ao meu lado durante esta jornada.

Ao Prof. Dr. Enrique Vilarrasa e a Profa. Dra Diana Cristina Silva de Azevedo, pela excelente orientação e, também, pela oportunidade, confiança e ensinamentos transmitidos durante todo o desenvolvimento desse estudo.

Ao professor Dr. Moisés Bastos Neto, pelos excelentes *feedbacks* durante a pesquisa.

À Dra Rafaelle Gomes Santiago, uma pessoa incrível e uma excelente profissional, que foi parte fundamental do desenvolvimento dos experimentos dessa pesquisa.

Aos colegas de laboratório pelo constante apoio no desenvolvimento das atividades.

Aos colegas da turma de mestrado, pelas reflexões, críticas e sugestões recebidas. Ao Programa de Pós-Graduação em Engenharia Química (PPGEQ) e ao Grupo de Estudos em Separações por Adsorção (GPSA) pela a oportunidade a mim concedida.

RESUMO

A captura de dióxido de carbono (CO_2) é um tema amplamente estudado, com métodos de captura e armazenamento de carbono (CCS) ganhando destaque, especialmente aqueles baseados em adsorção gás-sólido. No entanto, observa-se que a literatura ainda carece de estudos sobre os impactos dos contaminantes das correntes gasosas (NOx, SOx, umidade, etc.) na adsorção de CO_2. Isto posto, o presente estudo objetiva avaliar o impacto da presença de dióxido de enxofre (SO_2) na captura de CO_2, em condições análogas ao cenário pós-combustão de biomassa para geração de bioenergia. Para tal, foram coletados dados de adsorção da zeólita 13X *Binder Free* (13XBF), por meio de uma balança de suspensão magnética (MSB), ante diferentes correntes gasosas (CO_2, N_2, SO_2 diluído em He (4500 ppm), CO_2/SO_2 diluído em He (4500 ppm), CO_2/N_2). Observou-se que a presença de SO_2 na corrente gasosa reduz a capacidade de adsorção de CO_2 e N_2 na zeólita, o que pode estar relacionado com a redução das propriedades texturais após a adsorção de SO_2, pois foi observada uma redução de cerca de 35% do volume total de poros. Por fim, concluiu-se que, para as condições em estudo, tempos de contato de até 3 horas entre 13XBF e SO_2 diluído em hélio (4500 ppm) permitem a recuperação do material de partida, o que não foi possível após tempo de contato de 12 horas a 50, 70 ou 90 °C. Assim, observa-se a necessidade de pré-tratamento do fluxo gasoso antes de passar para tecnologia de captura de CO_2. Por fim, recomenda-se que estudos futuros sejam realizados para avaliar o tempo crítico para que a adsorção de SO_2 se torne irreversível e para entender o efeito de outros contaminantes presentes nos gases de combustão (como vapor de água, CO, NO_x), dada a lacuna identificada na literatura, e a utilização de ferramentas de simulação molecular para realizar um estudo a nível molecular para avaliar a competição entre CO_2 e SO_2.

Palavras-chave: gás de combustão; CCS; enxofre; peneiras moleculares.

ABSTRACT

Carbon dioxide (CO_2) capture is a widely studied topic, and Carbon Capture and Storage (CCS) methods are gaining prominence, especially processes based on gas-solid adsorption. However, the literature lacks studies on the impacts of contaminants from gaseous streams, such as NOx, SOx, and humidity, on CO_2 adsorption. The present study aims to evaluate the impact of sulfur dioxide (SO_2) on CO_2 capture under conditions analogous to the post-combustion scenario of biomass for bioenergy generation. For this purpose, adsorption data of 13X Binder Free (13XBF) zeolite were collected using a magnetic suspension balance (MSB), before different gas streams (CO_2, N_2, SO_2 diluted in He (4500 ppm), CO_2/SO_2 diluted in He (4500 ppm), CO_2/N_2). It was observed that the presence of SO_2 in the gas stream reduces the CO_2 and N_2 adsorption capacity of the zeolite. This reduction may be related to the decrease in textural properties after SO_2 adsorption, resulting in a reduction of about 35% of the total pore volume. Finally, it was concluded that contact times of up to 3 hours between 13XBF and SO_2 diluted in helium (4500 ppm) allow the recovery of the starting material. However, it was not possible to recover the starting material after a contact time of 12 hours at 50, 70, or 90°C. Thus, suggesting the need for pre-treatment of the gaseous stream before moving on to CCS Technologies. Therefore, it is recommended that future studies be conducted to evaluate the critical time for SO_2 adsorption to become irreversible and to understand the effect of other contaminants (such water vapour, CO, and NOx) present in combustion gases, given the gap identified in the literature, and utilization of molecular simulation tools to carry out a study at the molecular level to assess the competition between CO_2 and SO_2.

Keywords: flue gas; CCS; sulfur; molecular sieves.

.

LIST OF FIGURES

LIST OF TABLES

LIST OF SYMBOLS

q_i	adsorbed amounts of components i
q_j	adsorbed amounts of components j
b	adsorption affinity or Langmuir constant
q_e	Adsorption capacity at equilibrium (mol.g^{-1})
E	Characteristic energy of a system
13XBF	Commercial binder free 13X zeolite
13X	Commercial zeolite 13X
k	constant associated with the adsorption energy
ρ_{N_2}	Density of liquid nitrogen
ρ	density of the surrounding gas
n_i	effects of energy heterogeneity
S	Elemental sulfur
CNHS	Elementary chemical analyses of Carbon (C), Hydrogen (H), Nitrogen (N), and Sulfur (S)
n	energetic heterogeneity of the surface of the adsorbent
$S_{i,j}$	estimate the selectivity components i and j in the mixture
m_{exc}	Excess adsorbed mass
$K_{h,i}$	Henry's constant
R	ideal gas law constant (8.314 J.mol^{-1})
$Ƞ_i$	interactions between molecules of the same type
ΔH_{ads}	isosteric heat of adsorption
K	Kelvin
Δm_{ads}	mass difference between the mass at each pressure and the mass under vacuum (after regeneration)
q_{max}	maximum amount adsorbed
q_m	Maximum theoretical adsorption capacity for the formation of a monolayer (mol.g^{-1})
MOF	Metal organic framework
y_i	molar compositions of the components i in the mixture
y_j	molar compositions of the components j in the mixture
M_{N_2}	Molar mass of N_2 (28.09 $g.mol^{-1}$)
n_{P_0}	Number of moles adsorbed at a pressure P
ε	Polanyi potential
PEI	Polyethyleneimine
V_s	specific volume of adsorbent
T	temperature
$n_{P_{0(mic)}}$	Total amount of moles that can be adsorbed in the micropores.
P	total pressure
V_0	Total volume that can be adsorbed
a_i / b_i	Virial coefficients
V_{sc}	volume of suspended components
XPS	X-ray excited photoelectron spectroscopy
V	V volume that can be adsorbed at a given relative pressure P/P$_0$

1 INTRODUCTION

The constant emissions of carbon dioxide (CO_2) in the atmosphere have generated a constant debate around measures to mitigate its increasing concentration. Legal actions (Brasil., 2020; Comissão Europeia, 2019), technological (Bui *et al.*, 2018; Meng *et al.*, 2021) and international agreements aiming to reduce the impacts of anthropogenic actions on the environment.

In this context, the International Energy Agency - IEA (2021a) pointed out that in 2020, CO_2 emissions reached the highest concentration in the atmosphere of the last three centuries, with the energy generation sector responsible for most of the emissions.

Within this context, British Petroleum Co. (2022) highlighted in its annual report that, although efforts have been made to diversify the world energy matrix, more than 70% of global primary energy came from coal, oil, and gas.

In order to mitigate this problem, different methods of Carbon Capture and Storage (CCS) methods have gained prominence in the literature.

It is estimated that technologies associated with CCS are of fundamental importance for the fulfillment of environmental goals (Meng *et al.*, 2021; Yong *et al.*, 2002), such as help keep the rate of global warming between 1.5ºC and 2ºC, which is one of the main points of the Paris treaty (United Nations, 2015).

According to the Intergovernmental Panel on Climate Change – IPCC (2022), the use of bioenergy aligned with CCS technologies represents a promising path to stop the increase the planet's average temperature by 1.5ºC. Samanta et al. (2012) indicate that, for power plants based on fossil fuels, CO_2 capture technologies can be classified into pre-combustion, oxy-fuel technology, and post-combustion; which have different levels of maturity, advantages**,** and disadvantages (Cormos, 2016; Fogarasi; Cormos, 2017; Meng *et al.*, 2021).

Technologies aligned with CO_2 capture in post-combustion scenarios have as one of their main advantages the fact that they represent an end-of-line technology, which means it can be adapted to any existing industrial unit (Shaw; Mukherjee, 2022).

In this context, different technologies have been proposed, such as calcium loop, chilled ammonia, membrane separation, absorption and adsorption (Darde *et al.*, 2009; Neto; Szklo; Rochedo, 2021; Pera-Titus, 2014; Rege *et al.*, 2001). Among the processes mentioned, gas-solid adsorption has been increasingly over the years (Bastos-Neto; Azevedo; Lucena, 2020a; Joos; Swisher; Smit, 2013; Joss; Gazzani; Mazzotti, 2017; Li *et al.*, 2009; Meng *et al.*, 2021; Rouquerol *et al.*, 2014).

Adsorption processes with solid sorbents for cyclic capture of CO_2 are considered promising methods due to the high selectivity of CO_2 at low pressures, the reusable nature of the adsorbents and the low investment-cost (Ardila *et al.*, 2012; Nicodème *et al.*, 2018). Besides, solid sorbents are potentially less energy demanding than liquid absorption and are mature technologies in natural gas (Figueroa et al., 2013), and in the chemical industry.

Regardless of the technology used, Friberg; Sadokhina; Olsson, 2019a; Li et al., 2022; Samanta et al., 2012 highlight that carbon dioxide sequestration is quite challenging, as it is usually found at low pressures and subject to contaminants, such as NO_x, SO_x, and water vapor, which can significantly affect the performance of the system.

However, the literature still lacks studies on the impacts of gaseous stream contaminants (NO_x, SO_x, particulate matter, moisture, etc.) on carbon capture.

Studies focused on understanding the impacts of SO_2 and how affect the kinetics of the adsorption reaction are even rarer (Arakawa; Matsuda; Kinoshita, 1997; Dantas, 2019; Friberg; Sadokhina; Olsson, 2019b).

Given the literary negligence in understanding the impacts of gaseous stream contaminants in CCS technologies aimed at the energy sector, especially concerning bioenergy production, and knowing the importance of analyzing post-combustion scenarios, the present study has the general objective of evaluating the impact of sulfur dioxide (SO_2) on CO_2 capture, under post-combustion scenario conditions of biomass for bioenergy generation using adsorption data (single and multi component) in 13X Binder Free zeolite, and application of mathematical models to describe the equilibrium conditions.

Given the above, outlined the following specific objectives:

a) Evaluate the adsorption/desorption capacity of the 13XBF zeolite in relation to the capture of CO_2 and N_2, as well as the gaseous mixture between these components.

b) Determine the equilibrium parameters of monocomponent adsorption for CO_2 and N_2 from the adjustment of the Sips Equation, and estimate the isosteric enthalpy of adsorption for the mentioned components.

c) Evaluate the adsorption/desorption capacity of SO_2 diluted in He (4500 ppm) of the 13XBF zeolite, as well as the gaseous mixture CO_2/SO_2 diluted (4500 ppm He), at different temperatures (50, 70, and 90 ºC).

d) Determine the equilibrium parameters of monocomponent adsorption for CO_2 and N_2 after contact with diluted SO_2 (4500 ppm He), based on the adjustment of the Sips Equation, as well as estimate the isosteric enthalpy of adsorption for the mentioned components.

e) Understand the possible alterations suffered by zeolite 13XBF upon exposure to SO_2.

For this purpose, 13XBF zeolite was chosen as adsorbent, because, as pointed out by Lig *et al.* (2009)*,* this material is commonly used to separate CO_2 from combustion gases, in addition to being considered a standard reference material for adsorption studies.

Furthermore, the Sips model was used as a basis for the development of adsorption isotherms because it uses the energetic heterogeneity of adsorption sites as a parameter, making it more suitable for describing adsorption processes in which different adsorption sites have different affinities for adsorbate (Do, 1998; Sips, 1950)

Thus, the work was divided into 5 sections, the first being this introduction. In topic two, the theoretical basis of the present study is presented, divided into four subtopics: (i) Carbon Capture and Storage (CCS) Technologies, (ii) Presence of sulfur dioxide (SO_2) in the post-combustion scenario, (iii) Fundamentals of adsorption, and (iv) adsorption equilibrium. Section three presents the experimental design of the present study, as well as the equipment and materials used. In the fourth topic, the results obtained are discussed, followed by final considerations, which comprise the fifth chapter of the present study.

2 REVIEW

Climate change resulting from anthropogenic greenhouse gas emissions has led to the need to develop and implement innovative technologies to mitigate environmental impact.

In this context, carbon capture and storage (CCS) technologies have emerged as essential tools in the global effort to combat climate change by mitigating anthropogenic carbon dioxide (CO_2) emissions. The urgency of addressing climate concerns has driven extensive research and development, highlighting CCS as a key solution.

The present study aims to explain CCS technologies, as well the theoretical foundations that enable the effective capture of CO_2 present in the atmosphere while addressing the challenges inherent to CCS. Furthermore, the aim is to provide a theoretical framework on the fundamentals of adsorption and use of zeolites as adsorbent materials, as they are crucial information to understand CCS technologies.

2.1 Carbon Capture and Storage (CCS) Technologies

To achieve the targets set by the Paris treatment and limit the rise in the planet's average temperature to between 2ºC and 1.5°C (United Nations, 2015), Carbon Capture and Storage (CCS) technologies have been widely applied (Oxford Institute for Energy Studies, 2022).

According to the International Energy Agency (2021) it is estimated that, by 2050, about 40% of all CO_2 on the planet comes from the application of CCS in the electricity production sector. Figure 1 presents a holistic vision for the adoption of CCS greenhouses, aligned with the use of renewable energy sources, which can contribute to a gradual reduction of the greenhouse effect.

Figure 1 - Carbon Capture and Storage (CCS): Overview from 2020 to 2050 in power electric sector
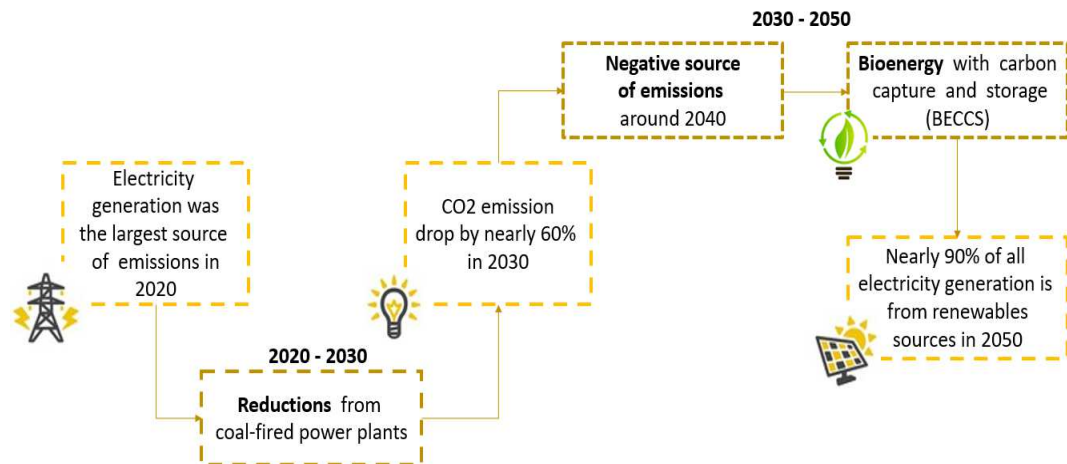
Source: Adapted from International Energy Agency (2021).

In the current energy scenario, the reduction of the carbon footprint is encouraged through the use of renewable energies and among them, the use of biomass has experienced notable growth. The choice and optimization of biomass combustion processes and installations to control polluting emissions has become an important research topic. Unfortunately, these combustion technologies release pollutants into the atmosphere, including CO_2.

Several techniques are in development for the separation of carbon dioxide from combustion flue gas streams, such as, cryogenic distillation, membrane, absorption, absorption process including pressure swing adsorption (PSA), vacuum swing adsorption (VSA) and temperature swing adsorption (TSA) (Yong, Mata, Rodrigues, 2002).

Traditionally, CO_2 capture has been carried out by absorption using chilled NH_3 or liquid amines (DARDE et al., 2009). Although this process is relatively inexpensive and achieves good CO2 capture rates, this strategy has drawbacks related to the high corrosivity of amines, low stability and the energy cost required for their reuse (Danckwerts, 1979). Furthermore, the energy consumed in separation by absorption represents 20% to 30% of the electric energy generated with the combustion (Song *et al.*, 2018)

Other methodologies, such as cryogenic distillation or membrane purification, have shown high CO_2 capture values in small-scale; however, the scale-up of these processes seem

to impair the capture efficiency or are too expensive to be competitive (Cabral; Mac Dowell, 2017; Pera-Titus, 2014).

For example, cryogenic processes are even more energy-intensive than absorption by amines and only economically competitive if a cheap low-temperature energy source is available (Song *et al.*, 2018). It is important to highlight that membrane processes are promising, but there are still long-term challenges to be overcome in selectivity and permeability (Yuan; Eden; Gani, 2016).

Nowadays absorption is the most mature CO_2 separation technique in post-combustion scenario, although research on CO_2 capture by adsorption is continuously growing to become an economically feasible alternative method.

Compared to absorption, adsorption processes with solid sorbents for cyclic capture of CO_2 are considered promising methods due to the high selectivity of CO_2 at low pressures, the reusable nature of the adsorbents and the low investment-cost (Figueroa *et al.*, 2008; Lee; Park, 2015).

Adsorption requires the use of a solid (adsorbent), packed in a column, either as fixed bed or fluidized bed, in which a gas mixture component is preferentially adsorbed.

Nevertheless, the applicability of this methodology depends essentially on the selection of the adsorbent and the regeneration strategy. In recent decades, the use of inorganic materials as adsorbents has emerged as a potential approach to capture CO_2 (Pera-Titus, 2014). Besides, solid sorbents are potentially less energy demanding than liquid absorption and are mature technologies in natural gas (Berg *et al.*, 2019) and in the chemical industry.

2.1.1 Use of solid sorbents to Carbon Capture and Storage (CCS)

Adsorption process is one of the most promising technology, as it potentially consumes less energy than absorption in liquids and is already industrially applied in both the natural gas industry (BERG *et al*., 2019) and the chemical industry.

In summary, an adsorbent material removes CO_2 from gas at a relatively low temperature in an adsorber. Once saturated, the adsorbent is fed to the desorber, where, with the aid of water vapor and at a higher temperature, CO_2 is regenerated in the form of a CO_2/water mixture that can be easily treated to obtain a stream of pure CO_2. The adsorbent regenerated in the desorber is recirculated to the adsorber.

In this context, temperature modulation adsorption technology (TSA) stands out, than is an energy-efficient and cost-effective a gas separation process that has gained significant attention recent years.

That technology involves the selective adsorption of a gas component on an adsorbent material at ambient temperature, followed by its release by heating the adsorbent to a higher temperature (Morales-Ospino, 2021).

The performance of TSA is highly dependent on the selection of the appropriate adsorbent material (Yu; Huang; Tan, 2012). Ideal adsorbent materials should have high selectivity, and high adsorption capacity from CO_2, while it must have high thermal stability.

In recent years, researchers have focused on developing novel adsorbent materials, including zeolites, metal-organic frameworks (MOFs), activated carbon, and mesoporous silica (Cui *et al.*, 2012; Kumar; Srivastava; Koh, 2020; Lee *et al.*, 2002; Merel; Clausse; Meunier, 2008; Morales-Ospino *et al.*, 2020).

2.2 Presence of sulfur dioxide (SO_2) in the post-combustion scenario

Sulfur dioxide (SO_2) is a prominent component in the post-combustion scenario, arising from the combustion of fossil fuels containing sulfur compounds. Its presence poses environmental and health concerns, necessitating effective mitigation strategies.

Upon entering the atmosphere, SO_2 stimulates the generation of acid rain by producing sulfuric acid (H_2SO_4). Moreover, it plays a role in the degradation of the ozone layer, intensifying the greenhouse effect (United States, 2024).

In the context of post-combustion, SO_2 is a byproduct released into the atmosphere during the burning of coal, oil, natural gas or biomass. It contributes to air pollution and forms acid rain, impacting ecosystems, human health, and infrastructure. Recognizing the adverse effects of SO_2 emissions, researchers have focused on developing advanced technologies for its capture and removal.

Recent studies have explored various post-combustion technologies aimed at mitigating SO_2 emissions. Sokolar and Nguyen (2022) discusses novel sorbent materials for SO_2 capture, emphasizing their efficiency and environmental benefits, standing out as promising solutions for efficient SO_2 capture.

One of the primary methods used in post-combustion FGD is wet scrubbing with alkaline solutions, such as limestone slurry or lime slurry (Srivastava, Jozewicz, 2001). In this process, the flue gas containing SO_2 is passed through an absorber tower where it comes into contact with the alkaline solution. The reaction between SO_2 and the alkaline solution forms calcium sulfite/sulfate, which is then oxidized to produce gypsum:

$$SO_2 + CaCO_3 + \frac{1}{2}O_2 + H_2O \rightarrow CaSO_4.2H_2O + CO_2$$
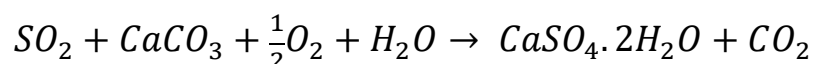
The gypsum produced as a byproduct can have economic value and find applications in various industries, including construction materials (Koralegedara *et al*., 2019). Wet scrubbing is known for its high efficiency in SO_2 removal, often exceeding 90%, making it a widely adopted technology in power plants and industrial facilities.

Another approach for flue gas desulfurization in post-combustion scenarios is dry sorbent injection (DSI), which involves injecting dry sorbents like sodium bicarbonate or hydrated lime directly into the flue gas stream (Zhang *et al*., 2022). The sorbent reacts with SO_2 to form sulfites/sulfates, which can then be captured using particulate control devices such as baghouses or electrostatic precipitators. While DSI is generally less complex and more cost-effective to install compared to wet scrubbers, it may have lower removal efficiencies, typically ranging from 50% to 80%.

Additionally, advanced FGD technologies such as seawater scrubbing and circulating fluidized bed (CFB) FGD have gained attention for their potential to achieve higher SO_2 removal efficiencies and reduce water usage (Koralegedara *et al*., 2019). Seawater scrubbing utilizes the natural alkalinity of seawater to absorb SO_2, while CFB FGD integrates FGD with a fluidized bed reactor, offering enhanced sorbent utilization and flexibility in handling different fuel types.

Despite the effectiveness of these FGD technologies, challenges such as waste disposal, energy consumption, and operational costs remain significant concerns (COLLS, TIWARY, 2009). Ongoing research aims to improve process efficiency, develop alternative sorbents with higher reactivity, and explore innovative approaches like membrane-based separation for SO_2 capture in post-combustion scenarios.

A pivotal aspect in the post-combustion scenario is the integration of SO_2 capture technologies into existing power plants. Research by Chen et al. (2021) highlights the challenges and opportunities of retrofitting SO_2 capture technologies into conventional power generation facilities, shedding light on the practical implications of implementation.

It is noteworthy that, despite the need and importance of removing SO_2 from the atmosphere, its capture is quite challenging, as this compound is commonly found alongside different elements, such as CO, CO_2, N_2, H_2O, and others, in concentrations frequently fluctuating between 500 to 5000 ppm (Moreira, 2022; Rackley, 2017).

However, it is observed that the literature has been scarce in terms of understanding the impacts of SO_2 (considered a contaminant of gaseous streams) on CCS technologies. That said, research focusing on the effects of sulfur dioxide on carbon capture systems is crucial for optimizing the efficiency of these processes, besides contributing to the development of

efficient and environmentally friendly technologies, addressing the challenges associated with SO_2 emissions.

2.3 Fundamentals of adsorption

Adsorption is a spontaneous and exothermic phenomenon which takes place when molecules of a fluid are attracted and retained on the surface of a solid. This phenomenon occurs whenever a solid surface is in contact with a fluid, and it is defined as the enrichment or increase in the density of the fluid at the interface (Rouquerol et al., 2014; Ruthven, 1984).

According to the nature of the forces that govern the phenomenon, we can classify adsorption as physical (physisorption) or chemical (chemisorption). Physical adsorption is governed by intermolecular forces between the adsorbate and adsorbent, while chemical adsorption implies the formation of new chemical bonds.

The specific molecular interactions found in physisorption (e.g., polarization, field-dipole, field gradient quadrupole) typically occur as a result of particular geometric and electronic properties of the adsorbent and the adsorptive (Thommes *et al.*, 2015). In cyclic separation processes, physisorption is preferred because it is easily reversed (desorption) upon temperature or pressure swings and the adsorbent may be reused.

2.3.1 Zeolites as adsorbent materials

There are several materials in the literature that can be used as solid adsorbents in gas adsorption systems, and characteristics such as microporosity, surface chemical composition, stability and capacity are extremely important for better adsorption.

Table 1 summarizes some of the main adsorbents mentioned in the literature.

Table 1 - Adsorbents Characteristics

Material	Characteristic	Reference
Activated Carbons (ACs)	High degree of porosity High internal surface Highly efficient CO_2 capture High thermal stability Low sensitivity to moisture	Oliveira et al. (2021); Ojeda-López et al. (2022);Sayari; Belmabkhout; Serna-Guerrero (2011).
Zeolites	Thermal stability High surface área Less susceptible to reactions that could lead to spontaneous combustion in the bed	Kumar; Srivastava and Koh (2020)

Table 2 - Adsorbents Characteristics (continuation)

Material	Characteristic	Reference
Metal Organic Frameworks (MOFs)	"Highly designable crystalline porous solids with interesting potentials but they have a low resistance to moisture and low chemical and mechanical stability"	Gutierrez-Ortega et al. (2022), p. 2
Silica-Based Materials	"Usually requires surface functionalization (i.e., amine grafting) for effective CO_2 capture. However, they suffer from sluggish regeneration and degradation over time, which limit their practical application."	

Source: prepared by the author (2023).

Among the adsorbents mentioned in

Table 1 zeolites are worth mentioning, as they are known for their affinity for carbon dioxide, especially natural zeolites, 4A, 5A, 13X, and Y (Mofarahi; Gholipour, 2014; Rufford *et al.*, 2012; Triebe; Tezel, 1995), commonly used to separate CO_2 from combustion gases, with a higher carbon dioxide adsorption capacity than the materials mentioned (Li *et al.*, 2009). Figure 2 shows the adsorption mechanism of zeolites.

Figure 2 - Adsorption mechanism of zeolites
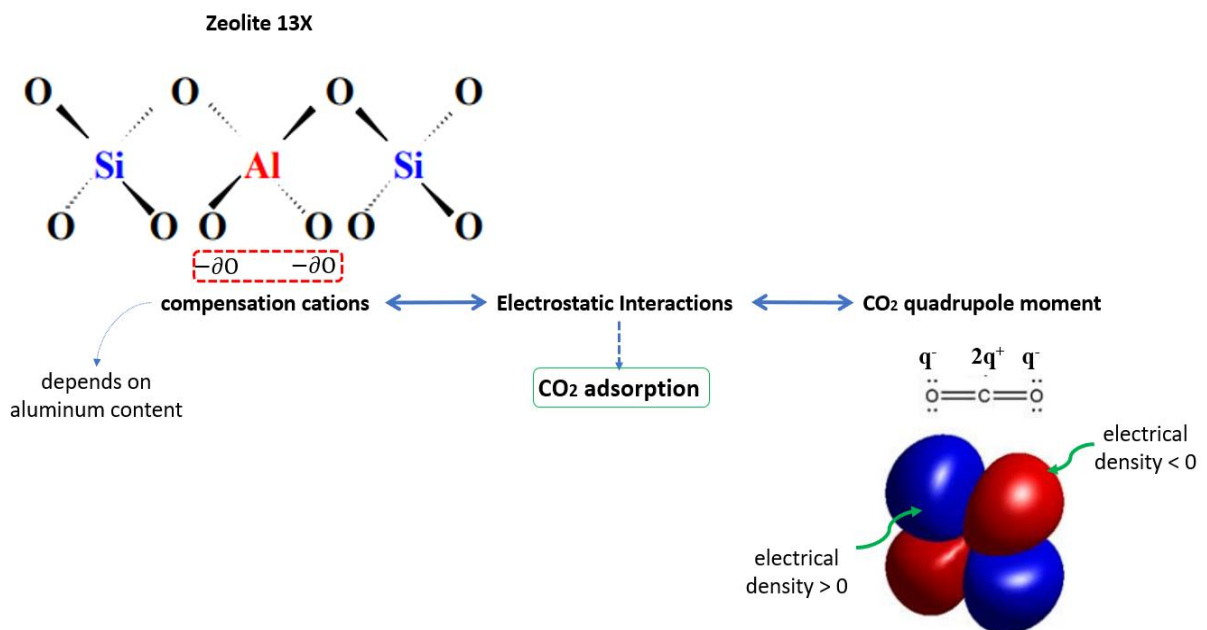
Source: Adapted from Cardoso (2016); Enzweiler; Coutinho; Schwaab, (2014); Júnior, (2017).

The quadrupole moment shown in Figure 2 shows a strong interaction with the electric field created by the zeolite compensation cations, so this material presents promising results for application in CCS Technologies (Morales-Ospino *et al.*, 2021).

Zeolites (also known as molecular sieves) are materials with a porous crystalline structure containing pores of molecular size (0.5-1.2 nm), as shown in Figure 3.

Figure 3 - Three-dimensional structure (13X Zeolite)
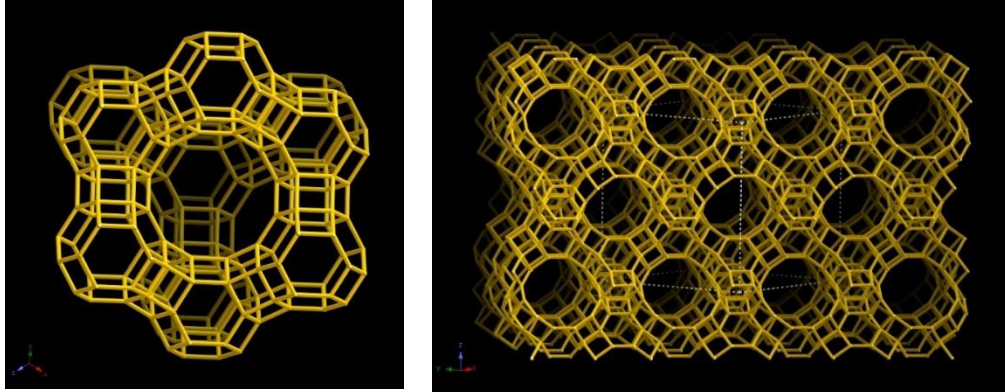
Source: International Zeolite Association (IZA).

For adsorption applications, zeolites are considered to be aluminosilicates of alkali or alkaline earth metals, such as Na, K and Ca (cationic). The typical structure of a zeolite is represented by the following general formula:

$$\{M_{x/n}[(AlO_2) \text{ x } (SiO_2)y] \cdot zH_2O\}$$
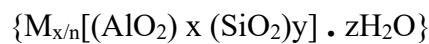
Where n is the valence of the cation, M is the cation, and z is the number of water molecules in each unit cell. The zeolite structures are networks made up of tetrahedral T atoms (T = Si, Al, etc.) bound by oxygen ions forming a crystalline framework that has cavities and pores of molecular sizes (Chester; Derouane, 2010).

The application of zeolites in the gas separation context is focused predominantly on the upgrading of natural gas and CO_2 capture in post-combustion scenario. Generally, zeolites have shown promising results for the separation of CO_2 from gas streams. CO_2 separation via zeolites is favored by the relatively large energetic dipole and quadruple of CO_2, which strongly interacts with the electric field created by the structural cations of zeolites (SAMANTA et al., 2012). On the other hand, heating rather than vacuum is required to desorb CO_2 from zeolites.

Among the different kinds of zeolites, zeolite 13X (faujasite) has been suggested as a promising adsorbent for CO_2 separation from flue gases due to its high adsorption capacity and thermal and mechanical stability (Bahamon; Vega, 2016; Harlick; Tezel, 2004). In addition, zeolite 13X remains today as a preferred adsorbent for industrial processes due to its availability on a large scale and costs (Morales-Ospino *et al.*, 2020).

2.3.2 Selectivy
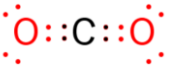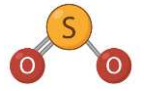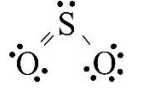
According to Dantas, (2019, p. 21), selectivity is an intrinsic characteristic of adsorbent materials, which "allows us to assess the preference for passing one [chemical] species over others".

In this context, this property is of paramount importance in the study of CO_2 capture from gaseous streams, as the different existing compounds have unique interactions with the adsorbent, which can substantially deviate from the idealized adsorption process (Murali; Sankarshana; Sridhar, 2013)**.**

Regarding the use of zeolites as adsorbent for CCS processes, Auerbach, Carrado, and Dutta (2003) point out that the adsorption capacity of a gas on a zeolite, whatever it may be, is a function of some intrinsic characteristics of the adsorbent, such as size, shape, and structure of the zeolite cavity, cationic charge density, concentration of cations, polarizability and permanent polarity of the zeolite. In general, a large or more polar gas molecule will be more strongly and selectively adsorbed on zeolites with smaller pores and higher cationic charge density.

In order to understand the influence on CO_2 capture, it is important understand why same contaminants are attracted to 13X zeolite. Thus, some characteristics are summarized in Table 3 (CO_2 and SO_2).

Table 3 - CO_2 and SO_2 characteristic

Molecular Formula	Structural Formula	Lewis Structure	Molecular Geometry	Angle	Polarity
CO_2			Linear	180º	Nonpolar
SO_2			Angular	119º	Polar

Source: by author (2024).

Table 3 are of fundamental importance to understanding how contaminants from gas streams can affect the CO_2 adsorption process and, consequently, the Carbon Capture and Storage (CCS) system, as discussed by Auerbach, Carrado, and Dutta (2003).

Thus, SO_2 molecules are more strongly adsorbed by zeolite as a function of their polarity, as they interact more strongly with the compensating cations of zeolite, shown in Figure 2, than the quadrupole moment of CO_2.

Finally, it is important to highlight that, in addition to the influence resulting from the chemical interactions between the adsorbent and the adsorbate, there is the selectivity imposed by the size of the channels (pores) of the zeolite (Uguina *et al.*, 1993). However, this property is commonly related to the use of molecular sieves as catalysts, as it is important that the reagent is able to enter all channels of the catalyst for a better reaction rate (Jia *et al.*, 2019; Smit; Maesen, 2008), although it also affects CCS systems.

2.4 Adsorption equilibrium

The adsorption equilibrium conditions of a given system are defined through the study of adsorption isotherms, a function of partial pressure (gases) or concentration (liquids) at a fixed temperature (WORCH, 2021), which are obtained experimentally, through equipment such as the magnetic suspension balance (MSB). "Adsorption equilibrium data provide the most important information for the understanding and design of adsorption processes" (Bastos‑Neto; Azevedo; Lucena, 2020b).

Given the intrinsic reaction mechanisms and financial infeasibility of get the isotherms experimentally the numerous conditions that an adsorption system may be subjected to, numerous mathematical models were developed with the aim of predicting the behavior of the system, based on the analysis and adjustment of parameters provided experimentally (Unuabonah; Omorogie; Oladoja, 2019). Figure 4 briefly presents the main phases of the adsorptive process, as well as the mathematical models addressed in the present study.

Figure 4 - Main phases of the adsorptive process and mathematical models[1]
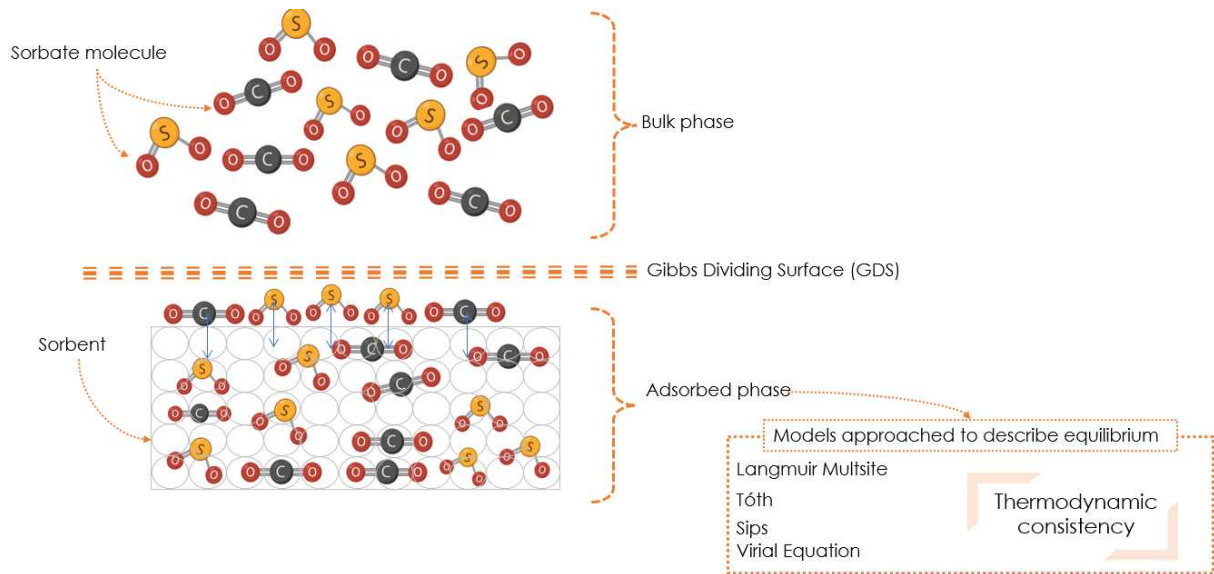
Source: by author (2023).

As shown in Figure 4, the present study is taken as a basis for the development of models mathematics that present thermodynamic consistency. This feature is of fundamental importance because it is coherent with the First Law of Thermodynamics, with Maxwell's relations and pressure and internal energy satisfying their definitions in terms of the Helmholtz free energy derivatives (Swesty, 1996).

In view of the above,

Table 4 presents the characteristic equations of the models addressed in this research.

Table 4 - Models approached to describe equilibrium

Item	Model	Equation[1]	Parameters specific		Reference
1	Langmuir	$q = \dfrac{q_{max}bp}{(1+bp)}$	-		Ruthven (1984)
1.1	Langmuir extended	$q = \dfrac{q_{max,i}b_ip_i}{(1+\sum_{i=1}^{j}b_ip_i)}$			
2	Sips	$q = \dfrac{q_{max}(bp)^{1/n}}{1+(bp)^{1/n}}$	n (dimensionle)	energetic heterogeneity of the surface of the adsorbent	Sips (1950)
2.1	Sips Extended	$q = \dfrac{q_{max,i}\left(b_i/\eta_i\right)p_i^{1/n_i}}{1+(\sum_{i=1}^{j}\left(b_i/\eta_i\right)p_j^{1/n_j})}$	η_i	interactions between molecules of the same type	Do (1998) e Sips (1950).
			n_i	effects of energy heterogeneity	

---

[1] "Gibbs dividing surface (or Gibbs surface) is a geometrical surface chosen parallel to the interface and used to define the volumes of the bulk phases in applying the foregoing definition to the calculation of the extent of adsorption, and of other surface excess properties" (IUPAC, 2002, p. 1).

Item	Model	Equation[1]	Parameters specific		Reference
3	Toth	$q = \dfrac{q_{max}bp}{\left(1+(bp)^n\right)^{1/n}}$	n (dimensionles)	energetic heterogeneity of the surface of theadsorbent	Toth (1971)
3.1	Toth extended	$q = \dfrac{q_{max,i}b_i p_i}{\left(1+\sum_{i=1}^{n}(b_j p_j)^{n_j}\right)^{1/n_i}}$			
4	Virial	$p_i = \left(\dfrac{q_i}{k_{h,i}}\right)^{(a_i q_i + b_i q_i^2)}$	a_i (kgmol^{-1}) b_i (kg^{2}mol^{-2})	Virial coefficients	Onnes (1911 *apud* Wisniak, 2012).
4.1	Virial extended	$p_i = \left(\dfrac{q_i}{k_{h,i}}\right)^{\left(\sum_{j=1}^{n} a_{ij}q_j + \sum_{j=1}^{n} b_{ij}q\right)}$	$K_{h,i}$ (molkg^{-1}bar^{-1})	Henry's constant	

Note([1]): p - pressure of the adsorbing species in the gas phase; b - adsorption affinity or Langmuir constant; q_{max} (mol.kg^{-1}) - maximum amount adsorbed.
Source: by author (2023).

In view of the equations presented in

Table 4, it is noteworthy that the mathematical models classified as extended refer to isotherms of gas mixtures, while the others are for single components.

Based on the adjustments of the single-component isotherms and after validating the models with the binary isotherms, it is possible to predict the adsorbed amounts of components i and j in the mixture and estimate the selectivity (Equation 1).

$$S_{i,j} = \frac{q_i y_j}{q_j y_i} \tag{1}$$

Where q_i and q_j are, respectively, the adsorbed amounts of components i and j in the mixture, and y_i and y_j are the molar compositions of the components in the mixture.

It is important to highlight that selectivity calculations were only developed for systems that reached equilibrium during the material's adsorptive capacity tests.

3 MATERIALS AND METHODS

The main goal of this study is to evaluating the impact of the presence of sulfur dioxide (SO_2) on CO_2 capture under post-combustion scenario conditions. To this end, the experimental design presented in Figure 5 was followed.

Figure 5 - Research design

1st step: understanding the adsorbent
- Determination of the adsorbent
- Characterization of the adsorbent: textural - specific surface area, total pore volume, micropore volume - CHNS, and XPS.

2nd step: single component adsorption studies
Determination of single components isotherms: CO_2, N_2, and SO_2 (4500 ppm in He).

3rd step: multi component adsorption studies
Determination of binary isotherms:
15% CO_2 + 85% N_2
20% CO_2 + 3% SO_2 (4500 ppm in He)

4th step: mathematical prediction of adsorbent amount
Equilibrium Models: Sips and Extended Sips.

Source: by author (2024).

The steps presented in Figure 5 are discussed in detail in subsequent topics.

3.1 Understanding the adsorbent

As shown in Figure 5, the first stage of the present study consisted of determining which adsorbent would be used to evaluate the impact of the presence of sulfur dioxide (SO_2) on CO_2 capture under post-combustion scenario conditions. To this end, search criteria were defined to consult the database (Scopus), thus delimiting the sample analyzed (Figure 6).

Figure 6 - Search parameters for adsorbent determination
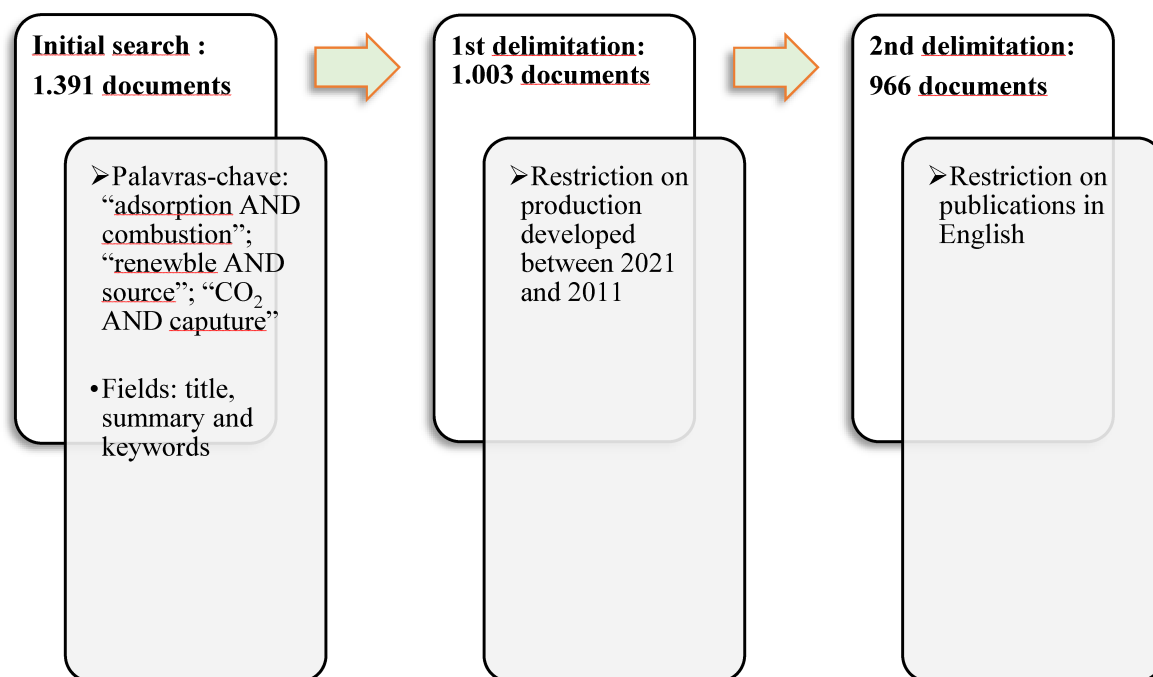
Source: by author (2024).

Based on the search parameters presented in Figure 6, the following solid adsorbents stood out:

- MOF (metal-organic structure),
- 13X zeolite,
- Polyethyleneimine (PEI), and
- Activated carbon.

It was decided to use zeolite 13X to the detriment of other adsorbents because 69,56% works used this material, reinforcing the above by Lig *et al.* (2009), this material is commonly used to separate CO_2 from combustion gases, in addition to being considered a standard reference material for adsorption studies.

Furthermore, some disadvantages of the most cited adsorbents in relation to zeolite 13X can be highlighted:

- MOF: more expensive to produce on a large scale and thermal regeneration can be more challenging compared to zeolites.
- Polyethyleneimine (PEI): recommended to chemisorption-based.
- Activated carbon: is not a competitive CO_2 adsorbent, when compared to MOFs and 13X zeolite)

The fundamental adsorption equilibrium data were obtained using the 13XBF (binder free) zeolite supplied by Chemiewerk Bad Köstritz GmbH (Germany) presented in the

form of beads with a diameter of 1.6-2.5 mm (Figure 7 (a)). Commercial zeolite 13X Zeolite (13X) from Shangai Hengye Chemical Industry, also in the form of beads, with a diameter average of 2 mm, as shown in Figure 7 (b).

Figure 7 – (a) Commercial binderless 13X zeolite (Köstrolith 13XBF) from CWK (Germany) and (b) Commercial zeolite 13X Zeolite (13X) from Shangai Hengye Chemical Industry
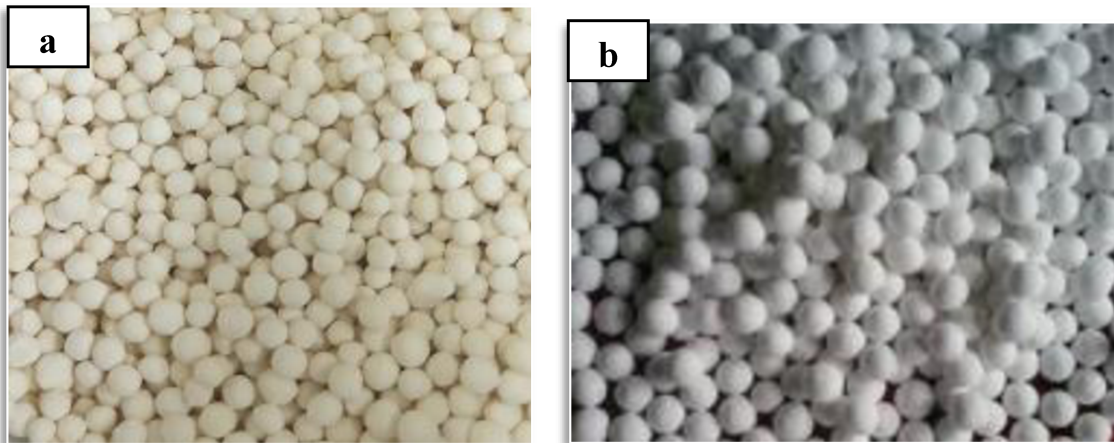
Source: by author (2024).

Regarding the textural characterization of the adsorbent (13XBF), the manometric adsorption method was used, generating N_2 adsorption/desorption isotherms at -196.15°C and CO_2 at 0 °C using the Autosorb-iQ3 equipment (Quantachrome Instruments, USA) shown in Figure 8.

Figure 8 - Autosorb-iQ$_3$

Source: Quantachrome Instruments (2024).

The gases used for textural characterization was CO_2 (99.999%) and N_2 (99.999%), all of them supplied by White Martins Praxair Inc. (Brazil).

The N_2 adsorption/desorption obtained using the equipment presented in Figure 8 was used to determine the total pore volume, total micropore volume, and specific surface area.

The total pore volume determination is accomplished by utilizing the N_2 adsorption isotherm at 77 K (196.15 ºC). To achieve this, one simply to ascertain the adsorbed volume at the highest relative pressure attained, i.e., at $P/P_0 \cong 1$, and then apply Equation 2.

$$\widehat{V}_{po} = n_{ads} \frac{M_{N_2}}{\rho_{N_2}} \tag{2}$$

Where n_{ads} is the number of moles adsorbed at the maximum relative pressure, M_{N_2} is the molar mass of N_2 (28.09 $g.mol^{-1}$) and ρ_{N_2} is the density of liquid nitrogen (0.809 $g.cm^{-3}$).

The micropore volume was calculated applying the Dubinin-Radushkevich (DR) equation to N_2 isotherm. The equation in its non-linear form is given by Equation 3.

$$q_e = q_m^{-(k\varepsilon^2)} \tag{3}$$

Where ε represent Polanyi potential; q_e means adsorption capacity at equilibrium (mol.g^{-1}), qm represent maximum theoretical adsorption capacity for the formation of a monolayer (mol.g^{-1}), and k means constant associated with the adsorption energy.

The potential de Polanyi (also known as Potential Theory of Adsorption) states that adsorption can be measured by balancing the chemical potential[2] of a gas near the surface and the chemical potential of the gas from a great distance (Polanyi, 1963).

Thus, this parameter (ε) provides valuable information to understand the reactivity and energetics of chemical reactions that occur at surfaces (Equation 4).

$$\varepsilon = RT ln \frac{P_0}{P} \tag{4}$$

Where R: real gas constant (8.314 J.mol^{-1}); and T: temperature on the thermodynamic scale (K).

---

[2] Potential energy that can be absorbed or released during a chemical reaction.

The parameter described in Equation 5 can be used to draw a characteristic curve concerning the volume that can be adsorbed at a given relative pressure P/P$_0$ and the total volume can effectively participate in the adsorption process.

$$\frac{V}{V_0} = \exp\left(\left[-\frac{\varepsilon}{E}\right]^2\right) \tag{5}$$

Where: V is the volume that can be adsorbed at a given relative pressure P/P$_0$, V_0 is the total volume that can be adsorbed, and E is the characteristic energy of a system ($E = \left(\sqrt{k}\right)^{-1} [kJ.mol^{-1}]$).

The union of equations (4) and (5) results in the DR model (Equation 6).

$$\log\left(\frac{V}{V_0}\right) = -Dlog^2\left(\frac{P}{P_0}\right) \tag{6}$$

D is an empirical constant of the equation.

By translating Equation 6 to the amount of adsorbed moles, Equation 7 is generated.

$$\log(n_{P_0}) = \log\left(n_{P_{0(mic)}}\right) - Dlog^2\left(\frac{P}{P_0}\right) \tag{7}$$

Where $\boldsymbol{n_{P_0}}$ is the number of moles adsorbed at a pressure P and $\boldsymbol{n_{P_{0(mic)}}}$ is the total amount of moles that can be adsorbed in the micropores. Expressing Equation 7 in relation to the amount of adsorbed moles is important to find the region where micropores exist.

To do this, draw a graph $\log(n_{P_0}) \times log^2\left(P_0/P\right)$ and look for the region between 10^{-5} and 10^{-4} of relative pressure (in which the micropores are located) and then Equation 8 is applied to find the volume of micropores.

$$\widehat{V}_{P_{0(mic)}} = n_{P_{0(mic)}} \frac{M_{N_2}}{\rho_{N_2}} \tag{8}$$

Regard to the calculation of specific surface area, the BET method was adopted. Proposed by Brunauer, Emmett, and Teller (1938), this method presents an extension of Langmuir's theory, allowing for greater adsorption capacity by considering the formation of multiple layers on the surface. This theory acknowledges that the forces involved in physical adsorption resemble those in liquefaction, such as Van der Waals forces. Thus, physical

adsorption is not confined to monolayer formation; instead, it can progress to the formation of multilayers on the adsorbent's surface.

To determine surface area by the BET method, linear regression analysis was used (Figure 9).

Figure 9 - Determination of surface area by the BET method using linear regression
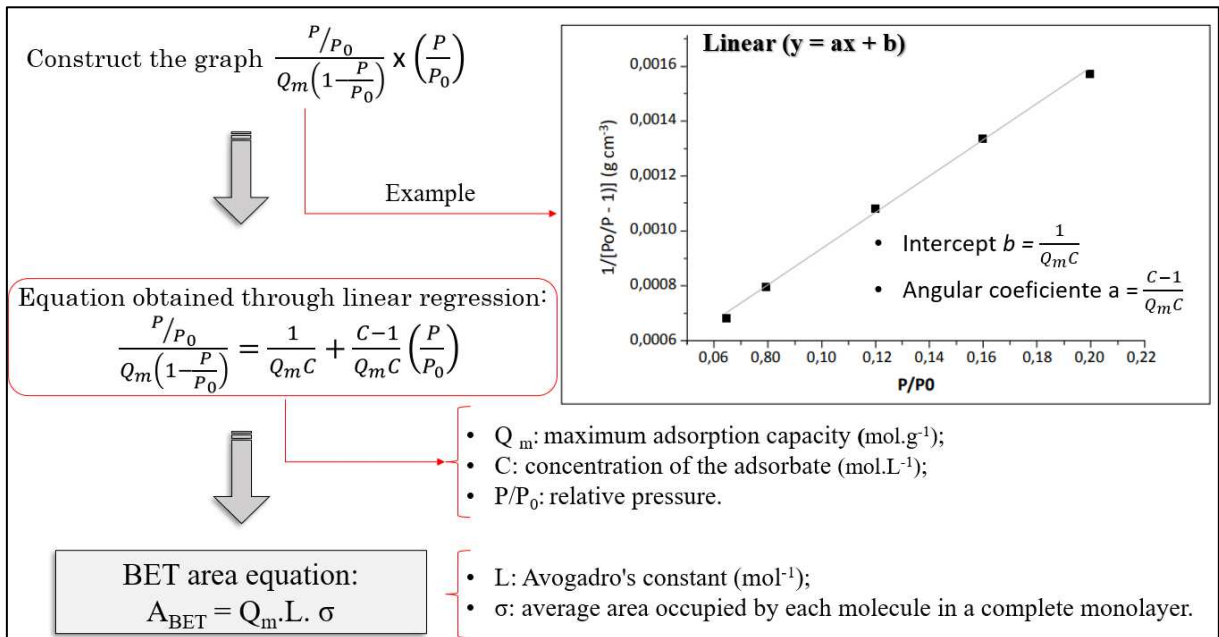
Source: Adapted from Nascimento *et al.* (2014).

In relation to the elementary chemical analyses of Carbon (C), Hydrogen (H), Nitrogen (N), and Sulfur (S), the equipment shown in Figure 10 was used to determine the quantity of these atoms in the 13XBF zeolite before and after contact with SO_2 (4500 ppm in He). The gases are separated through a gas chromatography column associated with a thermal conductivity detector. The percentages of elements are calculated based on the proportion of gases released about the incinerated matter.

Figure 10 - LECO CHNS 932 Elementary Analyzer

Source: Central Research Services - University of Malaga (2024).

Gases arising from the sample incineration process are separated through a gas chromatography column associated with a thermal conductivity detector. The percentages of elements are calculated based on the proportion of gases released about the incinerated matter. Such a relationship is only viable due to Proust's Law, which establishes that the elements that make up a pure substance are always the same and appear in a defined proportion.

Finally, in terms of X-ray excited photoelectron spectroscopy (XPS), the equipment shown in Figure 11 was used to determine the chemical composition of the 13XBF zeolite surface before and after contact with SO_2 (4500 ppm in He).

Figure 11 - Espectrómetro Multilab System 2000 Thermo Fisher Scientific

Source: Central Research Services - University of Malaga (2024).

The apparatus depicted in Figure 11 comprises an X-ray source, an energy analyzer for photoelectrons, and an electron detector. To conduct the analysis and identification of photoelectrons, it is imperative to situate the sample within a high-vacuum chamber. The indispensable requirement is that the excitation source be monochromatic, given that the energy of the photoelectrons is intricately linked to the energy of the X-ray. The electrostatic analyzer is tasked with scrutinizing the energy of the photoelectrons, whereas identification is executed through an electron multiplier tube or a multichannel detector.

3.2 Adsorption studies: single and multi component

As shown in Figure 5, the second and third stage of the present study consisted of single- and multi-component adsorption studies.

To this end, measurements of gas adsorption were carried out in a magnetic suspension balance (MSB) from Rubotherm (Bochum, Germany), with a mass resolution of 0.01 mg.

The experimental setup comprises the microbalance, the measuring cell, a data acquisition unit, a thermostat bath, an electric heater, and a vacuum pump. Figure 12(a) presents the components of the equipment used and Figure 12(b) the experimental setup.

Figure 12 – (a) Magnetic suspension balance (MSB) components and (b) experimental setup

A – Computer
B – Magnetic suspension balance (MSB)
C - Thermostat bath
D - Heating coil
E – Dosage control of gas mixtures
F - Gas e vapor dosing and pressure control systems
G - Vacuum pump
H - Gas reservoirs

Source: by author (2024).

Adsorption measurements were carried out with the following gases: He (99.999%), CO_2 (99.999%), N_2 (99.999%), and SO_2 (4500 ppm in He); all of them supplied by White Martins Praxair Inc. (Brazil). It is noteworthy that the SO_2 used in the experiments of the present study was already acquired from diluted in helium.

In this context, the adsorptive capacity of zeolite 13X (binder free) was calculated from Equation 9.

$$m_{exc}(p,T) = \Delta m_{ads}(p,T) + (V_s + V_{sc})\rho(p,T) \tag{9}$$

Where m_{exc} [g] denotes the excess adsorbed mass, V_s [cm^3] represents the specific volume of adsorbent, V_{sc} [cm^3] is the volume of suspended components in equilibrium, ρ [g.cm^{-3}] denotes the density of the surrounding gas, p [bar] is the total pressure and T [K] is the temperature, Δm_{ads} [g] indicates the difference between the mass at each pressure and the mass under vacuum (after regeneration).

The data provided by Equation 9 are of fundamental importance for the construction of adsorption isotherms, as summarized in the Figure 13.

Figure 13 - Sequence for the development of adsorption isotherms
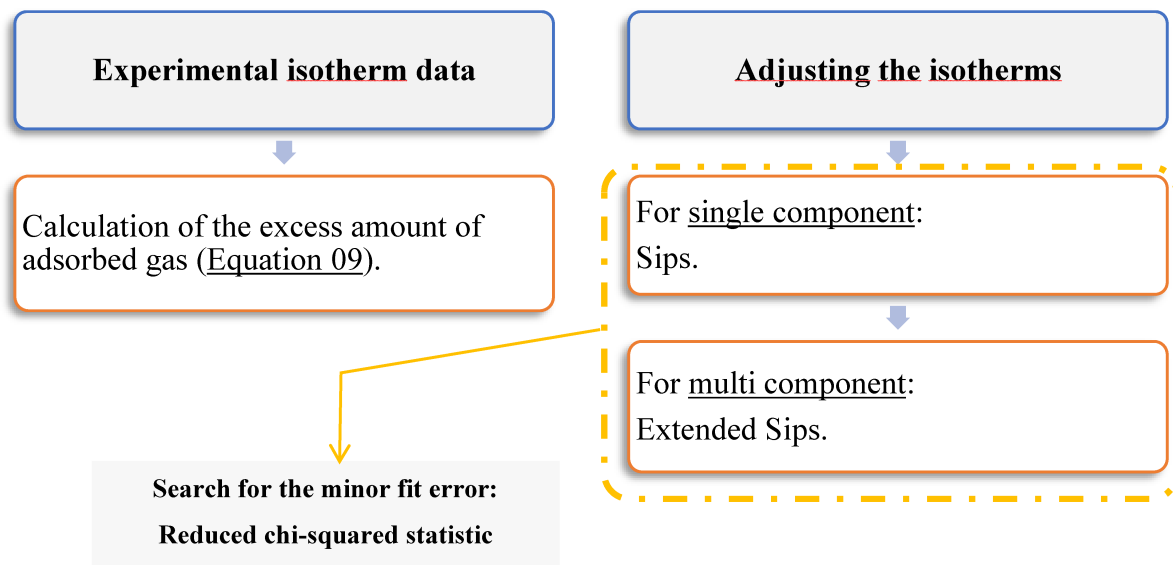
Source: by author (2024).

As shown in Figure 13, the Sips equilibrium model was initially tested, which presents an equation that combines the Freundlich and Langmuir isotherms, being valid to predict the behavior of heterogeneous adsorption systems (Bastos‑Neto; Azevedo; Lucena, 2020b).
When applied at low concentrations, the adsorption reduces to the Freundlich isotherm, while at high concentrations, the model predicts the adsorption in monolayers, which is a feature of the Langmuir isotherm (Bastos‑Neto; Azevedo; Lucena, 2020b). The equation that represents the Sips model is presented in

Table 4 (item 2).

The aforementioned model makes it possible to predict, from the adjustment parameters of monocomponent isotherms, the mixture isotherms, based on the extended models.

Furthermore, from the CO_2 and N_2 adsorption isotherms and using the Clausius-Clapeyron equation (Equation 10), the isosteric heats of adsorption were calculated.

$$\ln P = -\frac{\Delta Hads}{R}\left(\frac{1}{T}\right) + \text{constant} \tag{10}$$

Where P represents the pressure (bar), ΔH_{ads} is the isosteric heat of adsorption ($kJmol^{-1}$) and R is the ideal gas law constant ($R = 8.314$ $J.mol^{-1}.K^{-1}$).

Finally, Henry's constant is presented from a fresh sample of 13XBF zeolite, in order to evaluate the adsorption affinity between adsorbent and adsorbate. To this end, the Toth equation was used. Thus, the constant of Henry (K_h) has been calculated through Equation 11.

$$K_h = bq_m \tag{11}$$

Where K_h is Henry's constant, b represents the adsorption affinity, and q_m ($mol.kg^{-1}$) means the maximum amount adsorbed

In addition, based on the adsorption isotherms, the CO_2/N_2 selectivity was calculated.

Based on the methodology presented by Morales-Ospino (2021, p. 52) "in order to predict the amount adsorbed of component i ($i = CO_2$, N_2) in a binary mixture, an empirical approach using the Extended Sips model for n number of components (N_oC) has been applied", as described in

Table 4.

It is noteworthy to point out that, the gravimetric tests were performed with pure gas (CO_2 and N_2, White Martins, Brazil) and gas mixture (15% CO_2 and 85% N_2, 4500 ppm SO_2 in He).

Note the CO_2/N_2 gas mixture was carried out in situ using the gas mixture doser module (Figure 12 (b)), based on pure gases. On the other hand, SO_2 has already been purchased diluted, with no modification being made to obtain its mixture with He.

In view of the above, the characteristics of the research developed are discussed in the subsequent topics.

4 EXPERIMENTAL SECTION

4.1 Textural characterization

In order to decide which 13X commercial zeolite would be addressed in this study, the mentioned adsorbent was characterized with (13X) and without binder (13XBF), in the equipment shown in Figure 12. Tests were carried out with N_2 (at -196.15 ºC or 77 K). The isotherms obtained are shown in Figure 14 (a) and Figure 14 (b), respectively from zeolite 13X e zeolite 13XBF.

Figure 14 – N_2 adsorption/desorption isotherms at -196 °C for (a) 13X zeolite and (b) 13XBF zeolite. Empty symbols represent the desorption points.
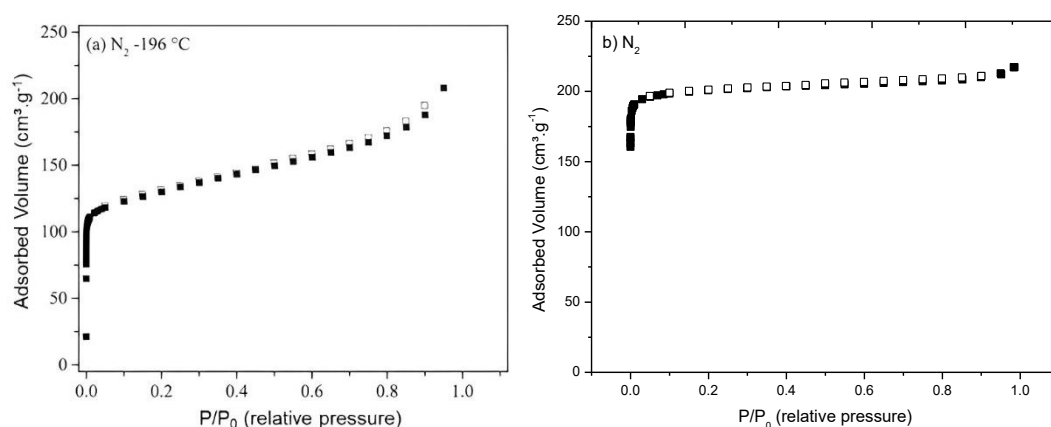
Source: by author (2024).

N_2 adsorption isotherms can be classified as reversible type I (a) according to the IUPAC classification (Thommes *et al.*, 2015), characteristic of microporous materials. Such information is consistent with data reported in the literature.

It is noteworthy that in relation to commercial zeolite 13X the typical constant plateau, normally observed in type I isotherms, is not reached. Instead, there is a steady, smooth increase in adsorption as relative pressure increases (Figure 14).

It is important to highlight that no hysteresis loop was observed,

The textural properties calculated from the adsorption isotherms represented in Figure 14 are summarized in Table 5

Table 5 -Textural properties obtained from N_2 adsorption-desorption isotherms at -196°C

Sample	Specific surface area* (m^2g^{-1})	Total pore volume (cm^3g^{-1})	Micropore volume (cm^3g^{-1})
13X	501	0.32	0.18
13XBF	829	0.34	0.31

Source: by author (2024).

In view of the data presented, it is observed that the commercial 13XBF zeolite presented superior textural properties than the 13X zeolite, both in terms of surface area and $V_{micropore}/V_{pore}$ ratio, which probably derives from a greater affinity with N_2.

Furthermore, aiming for greater robustness in the decision on which commercial zeolite X type would be used, the solid density, particle density, and particle porosity were analyzed, as these are crucial parameters for the simulation of adsorption processes (Table 6).

Table 6 - Adsorbent parameters: 13X zeolite binder free and 13X zeolite

Parameter	Relevance for process simulation	Equation	13X	13XBF
Solid density ρ_{sol} (kg.m^{-3})	Determine the amount of adsorbent material necessary to fill a given volume.	$\rho_s = \dfrac{1}{V_{sol}}$	2084	2263
Particle density ρ_p (kg.m^{-3})	Understand how adsorbent particles are packed in an adsorption bed or column.	$\rho_p = \dfrac{1}{(V_{sol} + V_{pore})}$	1250	1287
Particle porosity ε_p	Ability of the adsorbent to provide surface area for adsorption.	$\varepsilon_p = \dfrac{V_{poro}}{(V_{pore} + V_{sol})}$	0.40	0.43

Source: by author (2024).

In view of the data presented, it is observed that the 13XBF zeolite presents textural properties greater than 13X for all analyzed parameters. Therefore, it was decided to carry out the study using 13XBF zeolite as an adsorbent.

Finally, test was carried (**i**n the equipment shown in Figure 12) with 13XBF and CO_2 at 0 °C. The isotherm obtained is shown in Figure 15.

Figure 15 – Adsorption/desorption isotherms: for CO_2 at 0 ºC. Empty symbols represent the desorption points.
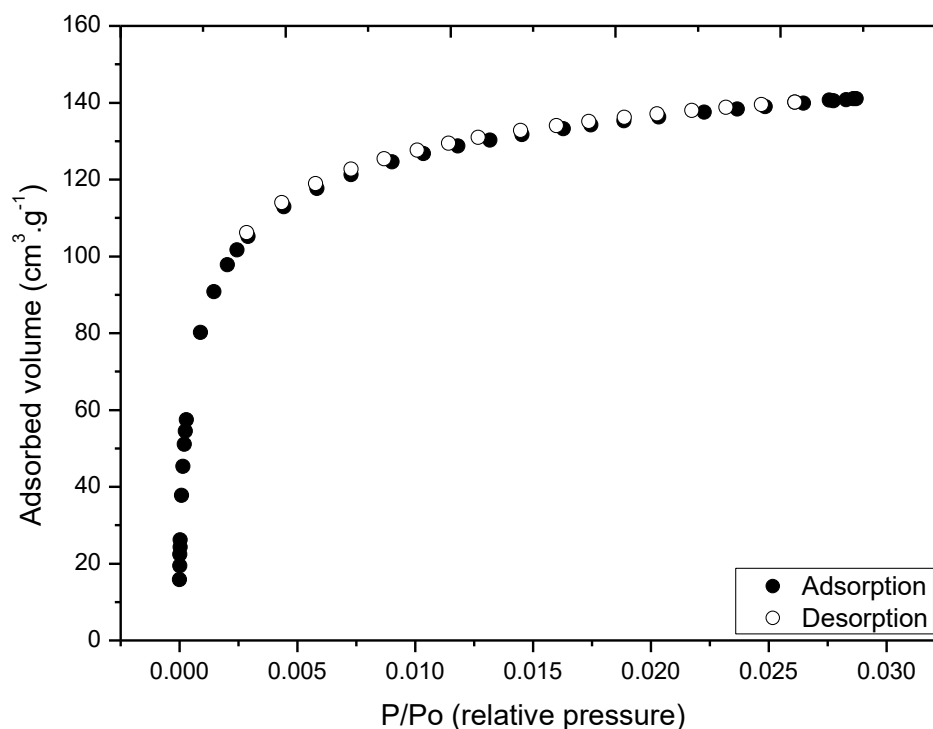
The CO_2 adsorption isotherms can be classified as reversible I(b) according to the IUPAC classification (Thommes *et al.*, 2015) characteristic of microporous materials.

The characterization of 13XBF zeolite was carried out with the pure gases CO_2 and N_2 because they have different molecular sizes and differences in molecular size can be relevant in contexts such as adsorption processes, where the molecular properties and size of the molecules can affect the interaction with materials adsorbents.

It is important to note that no hysteresis loop was observed, a fact that indicates that the material can completely desorb CO_2 all pressure ranges studied.

4.2 Adsorption measurements

Different models for isothermal equilibrium have been explored in the literature, and the Sips model was initially utilized for fitting experimental isotherm data owing to its accuracy and adaptability for extension to multicomponent mixtures (Ospino, 2018). The mathematical adjustment was show in Figure 16.

Figure 16 - Adsorption isotherms – Sips model for (a) CO_2 and (b) N_2.
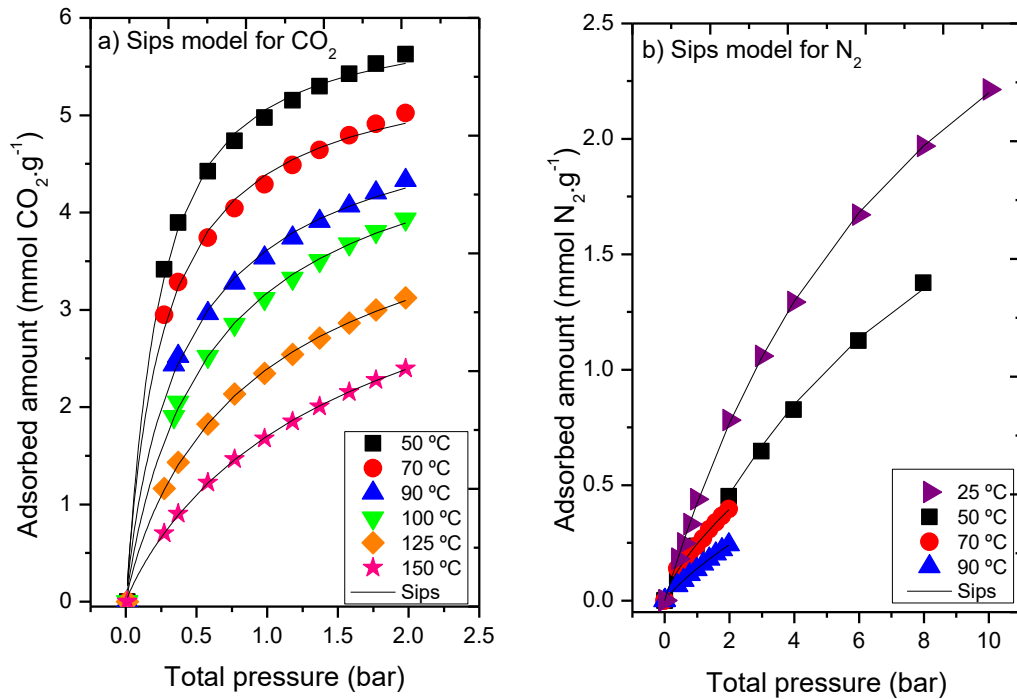
Source: by author (2024).

The data presented in Figure 16 (a) and Figure 16 (b) are consistent with other research in the literature, as Kim et al. (2016), Lee et al., (2002), and Morales-Ospino, (2021), and indicate that physical adsorption may be the main mechanism, since an increase in temperature results in a reduction in adsorption capacity.

It is important to highlight that the equilibrium models used showed good agreement with experimental data at all temperatures studied.

It is noteworthy that the isotherms presented in figure 16 were adjusted based on temperature, as shown in equations (12) to (14), and summarized in

Table 7.

$$q_{mi} = q_{moi} + X_i\left(\frac{1}{T} - \frac{1}{T_0}\right) \tag{12}$$

$$b_i = b_{oi}\,exp\left[\frac{Q}{R}\left(\frac{1}{T} - \frac{1}{T_0}\right)\right] \tag{13}$$

$$n_i = n_{oi} + k_i\left(\frac{1}{T} - \frac{1}{T_0}\right) \tag{14}$$

Table 7 - Adjustment parameters of Sips model of CO_2 and N_2 isotherms on 13XBF fresh

	Parameters					
	$q_{mi,0}$ (molkg^{-1})	X_i (K^{-1})	$b_{0,i}$ (bar^{-1})	Q (J.mol^{-1})	n_0	K (K^{-1})
CO_2	7,81	3845	14,24	25156	0,44	-451,3
N_2	7,04	7625	0,06	19945	1,00	0,0

Source: by author (2024).

Figure 16, enable to apply the Extended Sips model to make an estimation of the ideal CO_2/N_2 selectivity of all the samples at different pressure levels of the gaseous mixture.

From the adjustments of the monocomponent isotherms, it is possible to build the extended Sips models and compare the experimental data with the model predictions to validate the adjustments.

Thus, Figure 17 represent the binary CO_2/N_2 (15/85 v/v) isotherms and predictions of extended models, using the model of extended Sips.

Figure 17 - CO_2/N_2 mixing isotherms (15/85 v/v) for zeolite 13XBF - extended Sips model
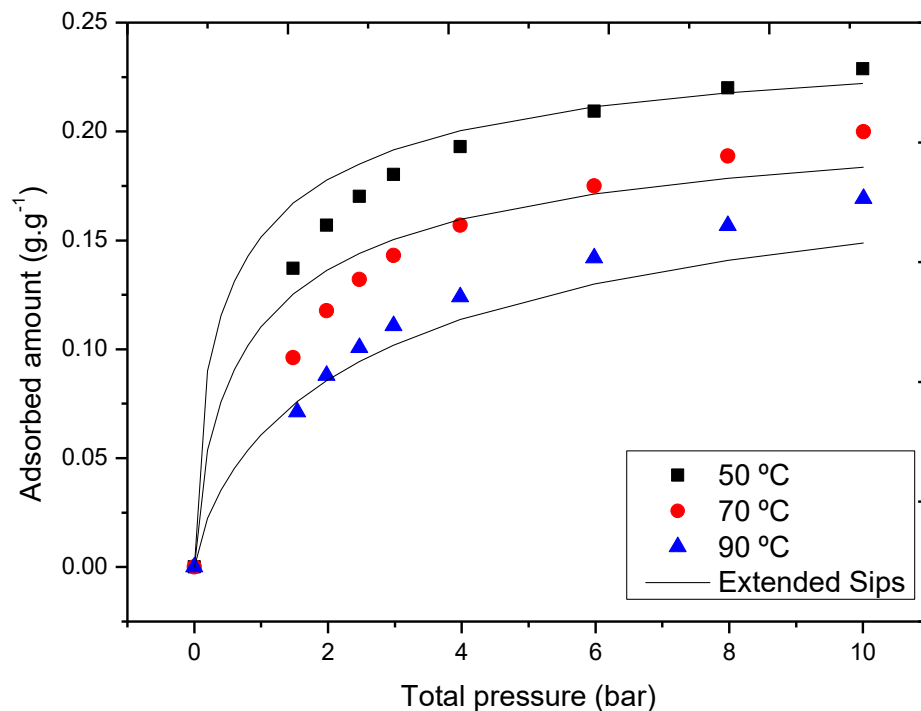
Source: by author (2024).

It is worth noting that the experiments related to estimating the adsorption capacity of 13XBF zeolite present as experimental limitations the lack of measurements in low-pressure regions. This is because the lowest pressure that the magnetic suspension balance (MSB) use is approximately 0.27 bar.

After evaluating the equilibrium model, it is possible to calculate the isosteric heat of adsorption of each component in the mixture predicted by the different equations.

It is noteworthy that the Clausius-Clapeyron equation is valid only if the adsorbate is physically adsorbed and when the system studied is at low pressures (Mateus, 2009). The isosteric heats of adsorption for CO_2, and N_2 were calculated using the adsorption data collected at 50, 70, and 90ºC (Figure 18).

Figure 18 - CO_2 and N_2 isosteric heats of adsorption
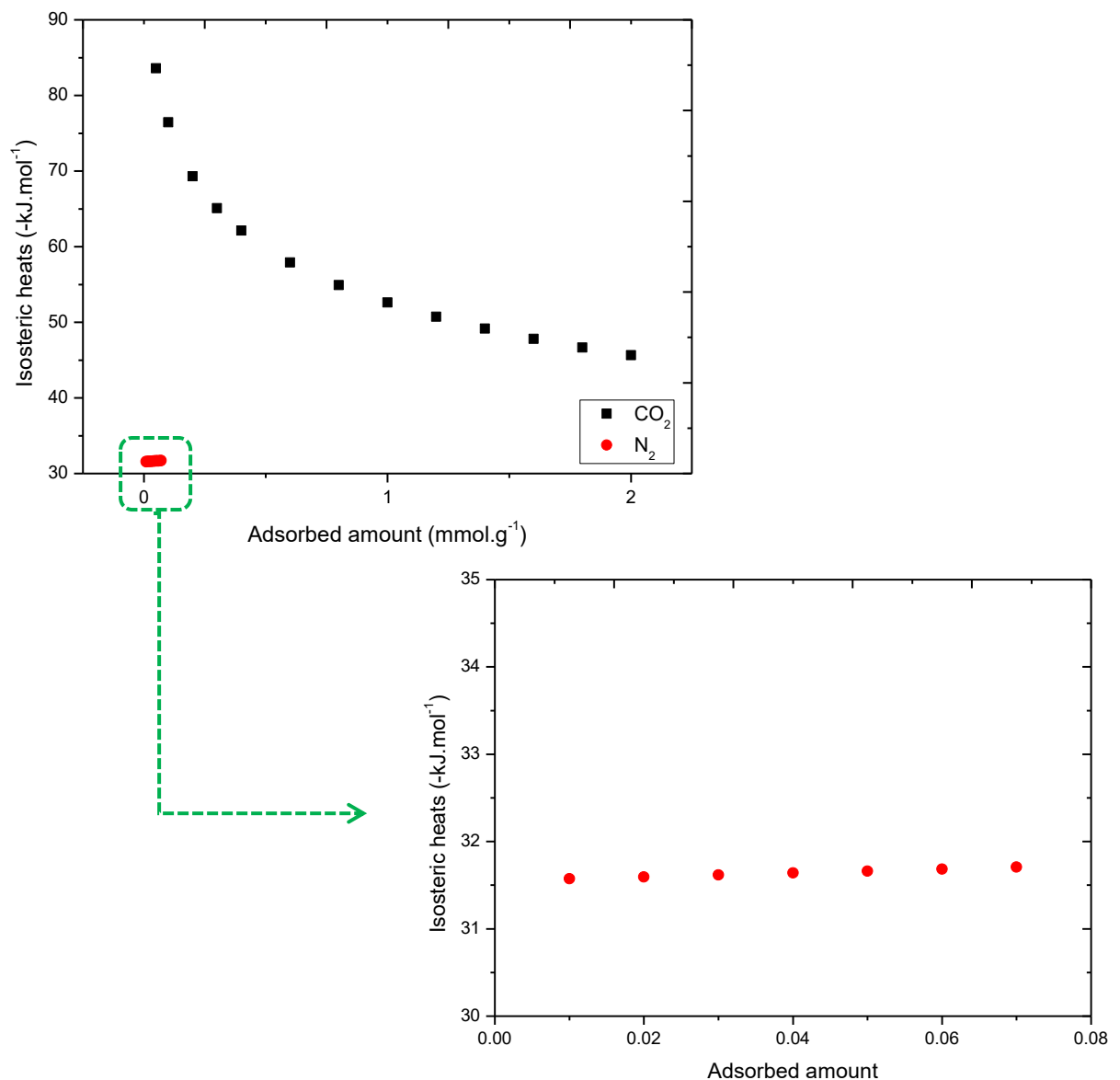
Source: by author (2024).

Values of the isosteric heat of adsorption, determined from Clausius Clapeyron equation or by direct calorimetry measurements, can provide a useful information into the

adsorption mechanism when taken together with data from adsorption isotherms (Rouquerol *et al.*, 2014).

Experimental studies have shown that the isosteric heat of adsorption of CO_2 on zeolite 13XBF is typically in the range of 90-30 kJ/mol (depending on the coverage), while the isosteric heats of adsorption of N_2 is almost constant (Cavenati; Grande; Rodrigues, 2004; Lee *et al.*, 2002).

The results (Figure 18) are consistent with the values found in the literature and indicate that CO_2 has a stronger interaction with the zeolite surface than N_2, which is expected given the higher polarizability and quadrupole moment of CO_2.

The decreasing profile of isosteric heat observed for CO_2 indicates an energetically heterogeneous surface, and the high value at low coverages is related to the strong interaction between the adsorbate (CO_2) and the strongest adsorption sites in the zeolite structure.

Knowledge of the adsorption equilibrium and isosteric heat of adsorption is fundamental for the proper design and operation of any gas-phase adsorption process, as it is a thermodynamic parameter that allows us to understand the adsorption mechanisms.

From Figure 18, it is evident that the heat of adsorption decreases as the adsorbed amount increases. This suggests an inhomogeneity on the surface, indicating that the most active centers are preferentially occupied initially. This observation is in line with the results documented in the literature (Gomes, 2014; Miano, 1996).

Furthermore, as a critical element in the design of adsorption processes, providing details on the heat released or absorbed during the adsorption or desorption processes respectively (H. Pan; J.A. Ritter; P.B. Balbuena, 1998; Shabbani, 2017).

The curves were adjusted to mathematical equations with the aim of having a tool that allows obtaining the isosteric heat of adsorption from the adsorbed quantity with greater precision. The fitting equations (Fitting Equation 15 (CO2) and 16) are compiled in Table 8.

Table 8 - Fitting equations for the isosteric heat of fresh sample 13XBF zeolite

Fitting Equation 15 (CO$_2$)	CO_2: ΔH (kJ mol^{-1}) = 14,026q^4 - 69,39q^3 + 123,41q^2 - 101,73q + 86,63 R^2 = 0,9944
Fitting Equation 16 (N$_2$)	N_2: ΔH (kJ mol^{-1}) = 31,5

Source: by author (2024).

Finally, Henry's constant is presented from a fresh sample of 13XBF zeolite, in order to evaluate the adsorption affinity between adsorbent and adsorbent (Table 9).

Table 9 - Summary of Henry's constant (K_h) from fresh sample of 13XBF zeolite

	50 ºC	70 ºC	90 ºC	100 ºC	125 ºC	150 ºC
CO_2	27.063	20.811	13.392	8.77	5.181	2.462
N_2	0.261	0.243	0.165			

Source: by author (2024).

Walton, Abney and Levan (2006) indicate that the higher the value of K_h, the higher adsorbent-adsorbate affinity. Thus, and based on Table 9, it is inferred that the selectivity of zeolite 13XBF is inversely proportional to the increase in temperature (Figure 19).

Figure 19 - CO_2/N_2 selectivity of fresh sample 13XBF at 50, 70 and 90º C
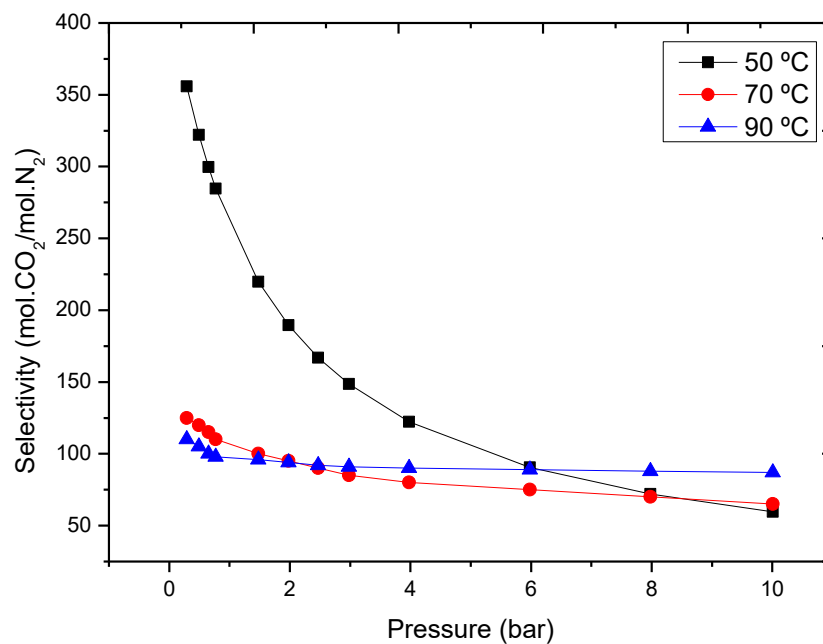
Source: by author (2024).

According to the data presented in Figure 19, it is possible to observe that the CO_2/N_2 selectivity, despite decreasing with increasing temperature, remains high for all pressure ranges studied.

The relationship between Henry's constant and the adsorption force of a zeolite can be understood in terms of the adsorption behavior of a gas in the zeolite. When a gas molecule is adsorbed into a zeolite, it interacts with the walls of the channels and cavities of the zeolite through various forces, such as Van der Waals forces, electrostatic forces, and hydrogen bonding (Ruthven, 1984).

The strength force of a zeolite is related to the strength of these interactions, which in turn affects the adsorption capacity and selectivity of the zeolite for different gases. Higher stoning forces generally lead to stronger adsorption and higher selectivity for specific gases.

In view of the data presented in Table 9, it is observed that as the temperature increases, the 13XBF zeolite has a lower capacity to adsorb the adsorbate molecules, a fact that is translated into CO_2/N_2 selectivity reduction as shown in Figure 19.

4.3 Adsorption SO$_2$ (4500 ppm in He) tests

After the adsorption tests of pure gases and gaseous mixtures, the impact of the presence of SO_2 on the gaseous stream to which the zeolite 13XBF was exposed was evaluated.

Initially, the sample was evaluated by adsorbed quantity curves of SO_2 diluted in He (4500 ppm) and evaluating the contact time of pre-adsorbed SO_2 in capturing CO_2, as well as the reversibility of the process.

To this end, the 13XBF zeolite was subjected to a constant flow of SO_2 diluted in He (4500 ppm) at 50 °C, up to a total pressure of 10 bar, allowing for 1, 2, 3, and 12 hours at each pressure step (Figure 20).

Figure 20 - SO$_2$ adsorption on 13XBF zeolite at 50 °C (4500 ppm SO$_2$ in He)). Empty symbols represent the desorption points
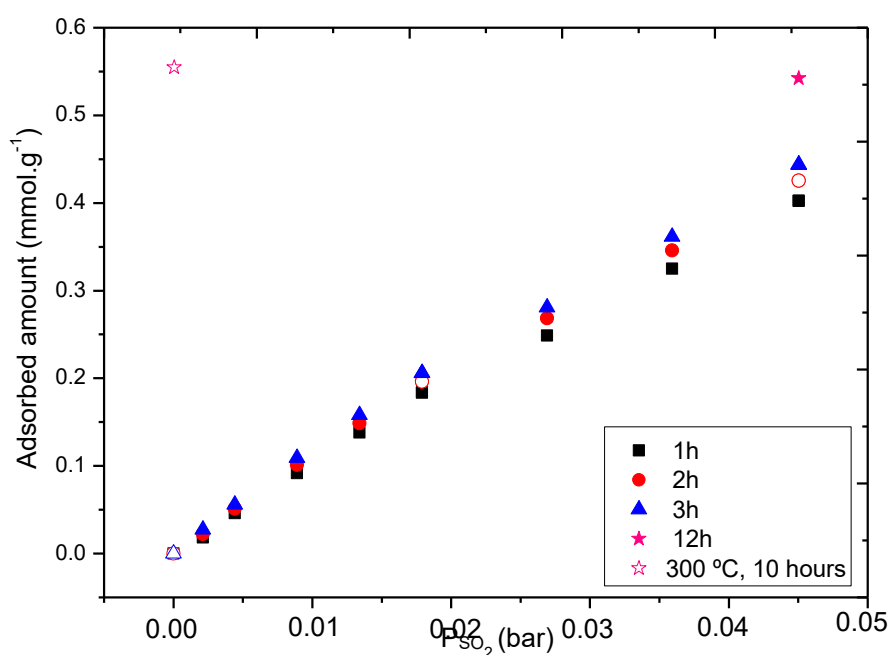
Source: by author (2024).

It is noteworthy that, for all cases presented in Figure 20, thermodynamic equilibrium was not achieved, as the amount of SO_2 adsorbed by 13XBF continued to increase proportionally to the period of exposure of the zeolite to the gas stream.

In this context, it is noteworthy that the SO2 adsorption process (4500 ppm in He) proved to be reversible for contacts of up to 3 hours between the adsorbent and the adsorbate, achieving, at least after 1 cycle, to recover the sample

A study carried out by Deng et al. (2012), using commercial 13X zeolite (13X) and concentrated SO_2 (99.9%), showed that this adsorbent has a greater affinity with SO_2 than with CO_2 and N_2.

Although the tests in this dissertation are carried out with SO_2 diluted in He (4500 ppm) the results found are consistent with those observed by Deng et al. (2012). This occurs due to the combined effect of diffusion effects in the outer surface and within the bulk of beads, in both types of zeolite (13X and 13XBF).

Another important aspect analyzed is the irreversibility of the process when the 13XBF zeolite is in contact with SO_2 (4500 ppm in He) for 12 hours. Thus, Figure 21 shows the amount of SO_2 adsorbed, at different temperatures, uptake 10 bar, and the remaining amount of such contaminant in zeolite 13XBF after degassing under vacuum (0.01 bar) at 300 °C for 12 hours.

Figure 21 - Remaining amount of SO_2 adsorbed after adsorption at (a) 50 °C, (b) 70 °C, (c) 90 °C, and regeneration at 300 °C for 12 hours. Empty symbols represent the desorption points.
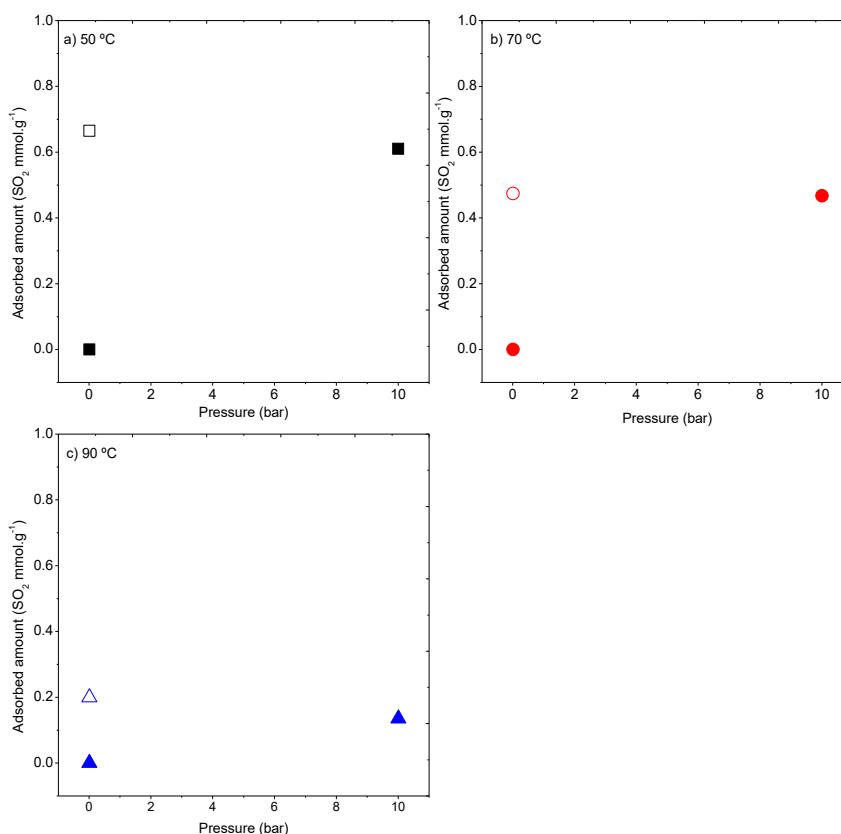
Source: by author (2024).

It is observed in Figure 21 that the SO_2 adsorption process proved to be irreversible at all temperatures studied after 12 hours of contact. After regeneration, an amount of retained SO_2 equivalent to that of adsorbed remains (10 bar, 4500 ppm SO_2 in He).

It is remarkable the slow adsorption kinetics of SO_2 when compared to CO_2. After 3 hours of contact the isotherm is reversible at the temperatures under study, managing to recover the sample. This phenomenon does not happen when the sample is in contact with SO_2 for 12 hours. After regeneration, an amount of retained SO_2 equivalent to that of adsorbed remains (total pressure 10 bar, 4500 ppm SO_2) This fact translates into a degradation of the sample, from the visual point of view (sample darkening) and, especially, in textural properties, as can be seen in Figure 22 (a) and Figure 22 (b), respectively.

Figure 22 - a) Change in the visual appearance of the 13XBF zeolite after contact with SO_2 (4500 ppm in He) and b) N_2 adsorption/desorption isotherms at -196 °C for Fresh Sample of 13XBF zeolite and after 12 h of contact with SO_2 (4500 ppm in He). Empty symbols represent the desorption points.
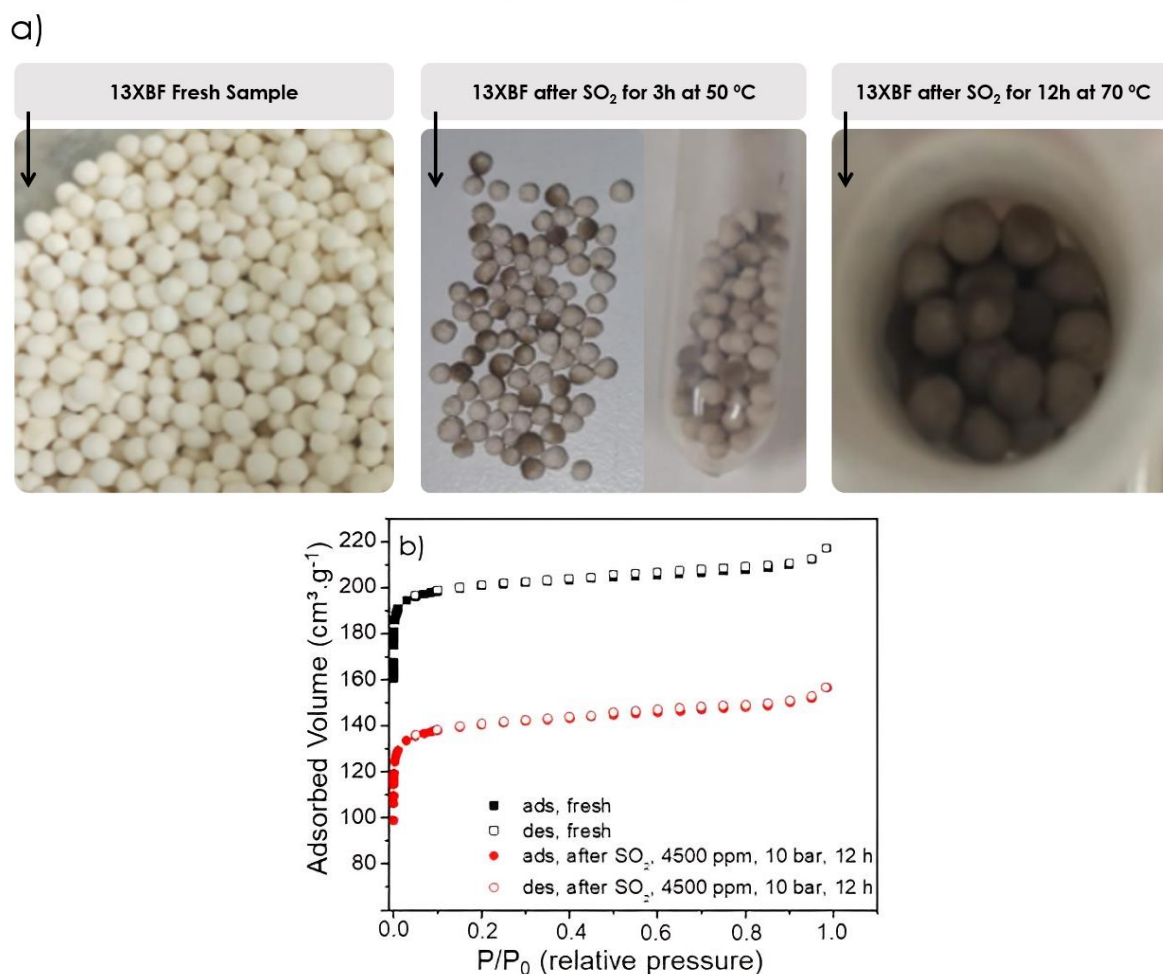
Source: by author (2024).

It can be seen from Figure 22(b) that, although there is a reduction in the amount of N_2 adsorbed at -196 °C, the shape of the isotherm remains constant, being classified as a type I isotherm according to the IUPAC classification (Thommes *et al.,* 2015), characteristic of microporous materials.

From the variations presented, to quantify the reduction in the textural properties of the material, the specific surface area, the total volume of pores and the total volume of micropores. Such data are presented in Table 10.

Table 10 - Textural properties obtained from N_2 adsorption-desorption isotherms at -196.15 °C before and after contact with SO_2 diluted in He (4500 ppm)

	Fresh sample	After contact with SO_2 (4500 ppm in He) for 12h	Reduction
Specific surface area* (m^2g^{-1})	829	566	31.7%
Total pore volume (cm^3g^{-1})	0.34	0.22	35.3%
Micropore volume (cm^3g^{-1})	0.31	0.21	32.3%

Source: by author (2024).

The variations shown in Table 10 can be attributed to the inability to desorb the SO_2 molecules from 13XBF under the studied conditions, indicating that this species is irreversibly adsorbed to the active sites of zeolite. Thus, there is a reduction in textural properties as compared to fresh 13XBF, because the pores of the material are already obstructed by SO_2 molecules. This observation is consistent with the findings of Yang et al. (2018) and Wijayanti et al. (2015).

To verify the presence of S species in the 13XBF zeolite as well as the chemical surroundings of these species on the zeolite surface, the virgin sample and after contact with SO_2 (4500 ppm in He) was studied by elemental analysis (CHNS) and X ray photoelectron spectroscopy (XPS). The results of the elemental analysis are presented in Table 11.

Table 11 - CNHS analysis results: samples before and after contact with SO_2. After contact with SO_2 (4500 ppm in He), the sample was regenerated with vacuum (13XBF (SO_2, 12 h)), and with vacuum and temperature at 300 °C for 12 h (13XBF, 12h, T).

	%C	%H	%N	%S
Fresh Sample	0.190	2.450	0.000	0.000
13XBF (SO2, 12 h)	0.254	2.256	0.000	0.242
13XBF (SO2, 12h, T)	0.217	2.232	0.000	0.166

Source: by author (2024).

From the results of elemental analysis (Table 11), it is possible to observe that after contact of the samples for 12 hours with SO_2 (4500 ppm in He) a certain amount of S species remains adsorbed on the 13XBF zeolite.

Thermal treatment at 300 °C for 12 hours under vacuum reduces the S present in the zeolite by approximately 25%. When the 13XBF zeolite was subjected to a flow of SO_2 diluted in He for 3 hours, after heat treatment, the presence of S species was not observed by elemental analysis, which is consistent with the preservation of the textural properties and the reversibility of the process pointed out in Figure 20.

Furthermore, given the need to know the chemical environment of the sulfur species (S) detected through CNHS analysis, we proceeded with X-ray photoelectron spectroscopy – XPS Figure 23.

Figure 23 - XPS analysis results: samples before and after contact with SO_2. After contact with SO_2 (4500 ppm in He), the sample was regenerated with vacuum (13XBF (SO_2, 12 h)), and with vacuum and temperature at 300 °C for 12 h (13XBF, 12h, T).
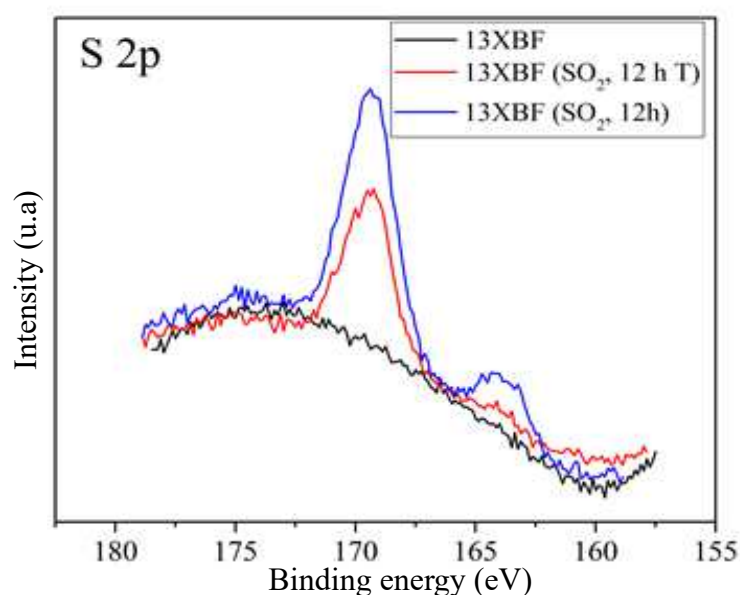
Source: by author (2024).

From Figure 23 it can be seen that the 13XBF sample does not present S species on its surface. After contact with diluted SO_2 (4500 pp in He) for 12 hours, a certain amount of S species is detected.

It is important to highlight that when the regeneration of the sample (after contact with SO2 diluted in He) is carried out solely by the application of vacuum, two contributions of S are detected, the one with higher binding energy associated with species with a higher

oxidation state, probably sulfate ions, while the one with the lowest binding energy is elementary S.

When the sample is subjected to heat treatment (300 °C under vacuum), both contributions continue to be observed, practically maintaining the proportion between them, as shown in Table 12.

Table 12 - XPS analysis results: samples before and after contact with SO_2 (4500 ppm in He)

	C1s	O1s	Na1s	Al2p	Si2p	S2p	S(%)/sulfate(%)
13XBF fresh sample	19.42	48.15	8.13	10.46	13.51	0.00	-
13XBF (SO_2, 12 h)	24.56	45.56	4.22	9.75	14.00	1.56	19/81
13XBF (SO_2, 12h, T)	23.35	47.83	3.96	9.26	13.88	1.44	18/82

Source: by author (2024).

As shown in Table 10, both elemental S and sulfate ions remain chemically adsorbed on the zeolite surface, and only a small portion of these species is removed after 12 h at 300 °C under vacuum.

Results similar to those found were published by Shi et al. (2015), who studied the combined adsorption of H_2S and SO_2 on activated carbon and observed a redox reaction, whose reaction products were elemental S and sulfate species, which were chemically adsorbed on the carbon surface and remained after heat treatment.

In this context, Sigot, Ducom, and Germain, (2016) when researching the mechanisms of sulfur retention in type X zeolite, based on the adsorption of H_2S, identified that the formation of elemental sulfur limits the thermal regeneration, suggesting that chemisorption is one of the mechanisms of adsorption present.

This fact can justify the data presented in Table 10, in which the proportion S(%)/sulfate(%) is practically the same, despite the sample being subjected to heat treatment at 300 ºC for 12 hours under a vacuum.

Furthermore, the finding of the formation of elemental sulfur justifies the reduction in the textural properties of the 13XBF zeolite, as when this chemical species is produced, it is primarily deposited on the pore walls and, depending on the size of the pore, may end up completely blocking the entry. This observation is consistent with Bagreev, Rahman, and Bandosz, (2001); and Sigot, Ducom, and Germain, (2016) studies.

In addition, to evaluate the effect of temperature of SO_2 adsorption on 13X zeolite, 13XBF was subjected to a constant flow of SO_2 diluted in He (4500 ppm) at 50, 70 e 90 °C up to a total pressure of 10 bar for 12 hours (Figure 24).

Figure 24 – SO_2 adsorption on 13XBF zeolite at 50, 70 and 90 °C (4500 ppm SO_2 in He) for 12 hours. Empty symbols represent the desorption points
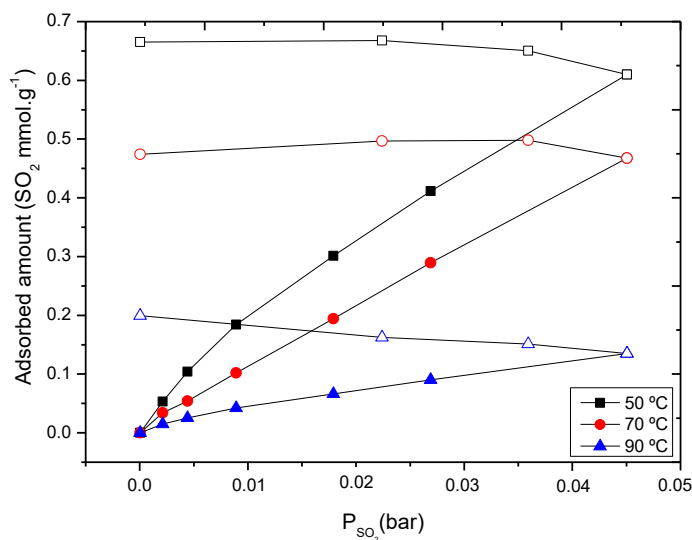
Source: by author (2024).

It can be seen from Figure 24 that the adsorbed amount drastically reduces with increasing temperature.

During experimental tests, the temperature of the reaction medium immediately increases when 13XBF comes into contact with SO_2. With the rapid rising in temperature, there is an increase in the amount of collisions between the gas particles and with the walls of the adsorbent, causing a disordered movement of the gas molecules (Mendes, 1995).

Thus, the access of SO_2 to the adsorption sites of 13XBF is not done efficiently, which can cause slower adsorption kinetics.

CO_2+SO_2 (4500 ppm in He) mixture was evaluated in the fresh zeolite at temperatures of 50, 70, and 90 °C. However, it was not possible to reach equilibrium under the studied conditions, consequently, there was no way to apply equilibrium equations.

Thus, the experimental data obtained through the gas mixture of 20% CO2 + 3% SO_2 (4500 ppm in He) at different temperatures (50, 70, and 90 °C) are presented (Figure 25).

Figure 25 - 20% CO_2 + 3% SO_2 (4500 ppm in He) adsorption curves for fresh zeolite 13XBF before any contact with SO_2 (4500 ppm in He). Empty symbols represent the desorption points.
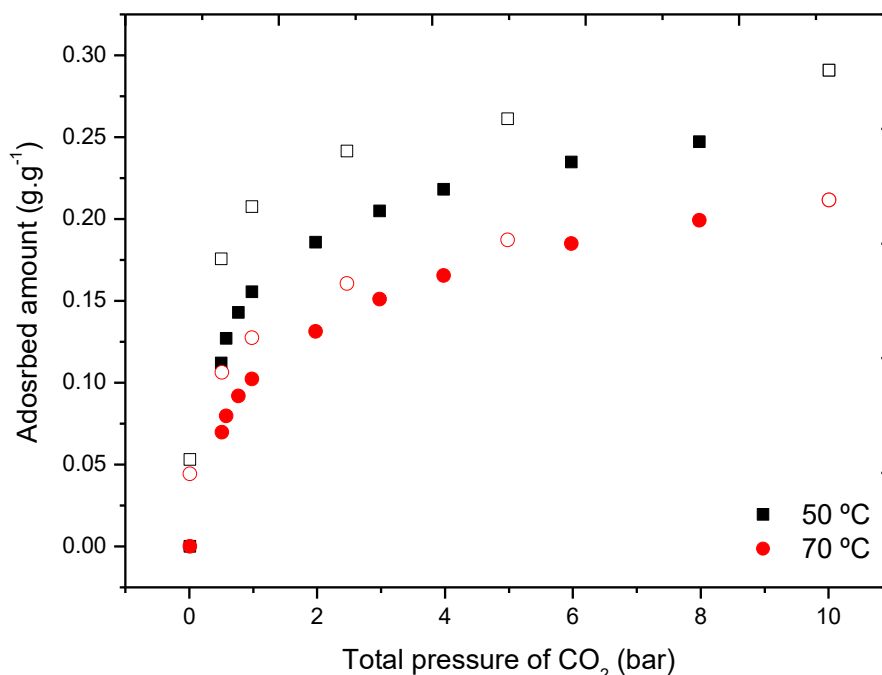
Source: by author (2024).

It is important to emphasize that the data presented in Figure 25 are consistent with the results presented in this study regarding the reversibility of the process. It was not possible to completely desorb the SO_2 adsorbed. Furthermore, the presence of hysteresis can be seen in Figure 25.

The presence of hysteresis loops in a given system may indicate that the bonds between the adsorbent and the surface groups of the zeolite are extremely strong, requiring a significant amount of energy to break them, thus resulting in a hysteresis between adsorption and desorption.

Such observations are consistent with the findings of the present study regarding the chemical species adsorbed on the surface of the 13XBF zeolite, as greater energy is required to desorb elemental S.

In addition, it is observed (Figure 25) that the adsorbed/desorbed amounts are not proportional to the increase in temperature and pressure. However, present a similar pattern of behavior at each temperature studied.

The SO_2 contact, even at low partial pressures, but for a prolonged period of time, (12 hours, for this study) leads to a decrease in the textural properties of 13XBF zeolite, which, as we will see below, translates into a loss of CO_2 adsorption capacity.

Given the above, it is possible to observe a significant reduction in the CO_2 adsorption capacity of the 13XBF zeolite when exposed to the contaminant under study (SO_2), especially if both gases ($CO_2 + SO_2$) are simultaneously present in the gas stream.

This observation is in line with the studies by Auerbach, Carrado, and Dutta (2003), who point out that the 13X zeolite has a greater affinity for SO_2 given the polarity of the molecule (CO_2 is nonpolar), in addition to interacting more strongly with the compensating cations of the zeolite than the quadrupole moment of CO_2 (Figure 2).

It is noteworthy that, in addition to the influence resulting from the chemical interactions between the adsorbent and the adsorbate, there is the selectivity imposed by the size of the channels (pores) of the zeolite (Uguina *et al.*, 1993).

Furthermore, in addition to analyzing the impact of temperature on the adsorptive/desorption capacity of the 13XBF zeolite, it is important to understand the impact of different forms of SO_2 contact with adsorbed.

It is known that one of the advantages of using adsorption as a basis for carbon capture and storage (CCS) technologies is the reuse of the adsorbent. However, for this to be possible (and for the system to maintain its efficiency) it is essential to understand the adsorbent stability.

Thus, given the need to understand the different ways in which the adsorbent has contact with contaminants in gaseous streams, the experimental steps shown in Figure 26 were outlined.

Figure 26 - Comparison of different forms of contact between SO_2 and zeolite 13XBF
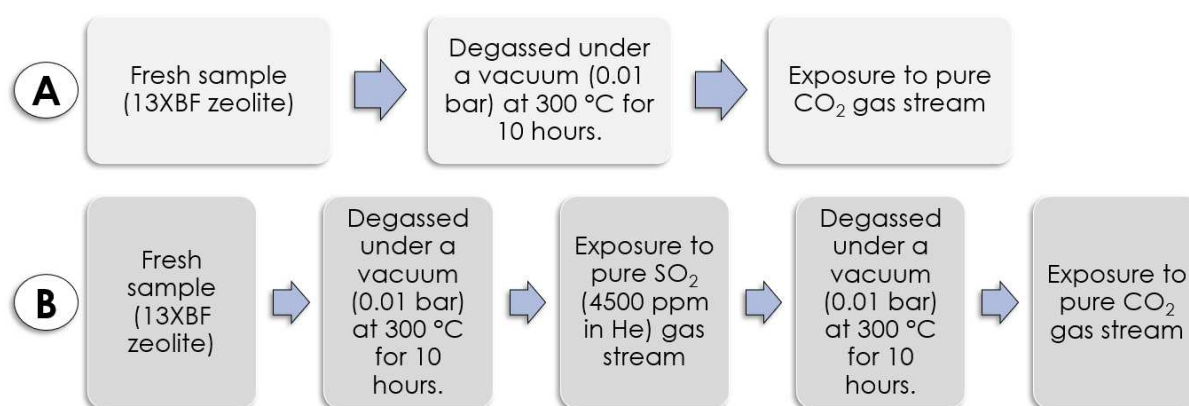
Source: by author (2024).

The data collected from the scenarios described in Figure 26 are shown in Figure 27.

Figure 27 – Comparison of the (a) CO_2 and (b) N_2 adsorption/desorption capacity of zeolite 13XBF when exposed to gaseous streams of CO_2 or N_2 before and after contact with SO_2 diluted in He (4500 ppm) at 50, 70, and 90 ºC. Empty symbols represent the desorption points.
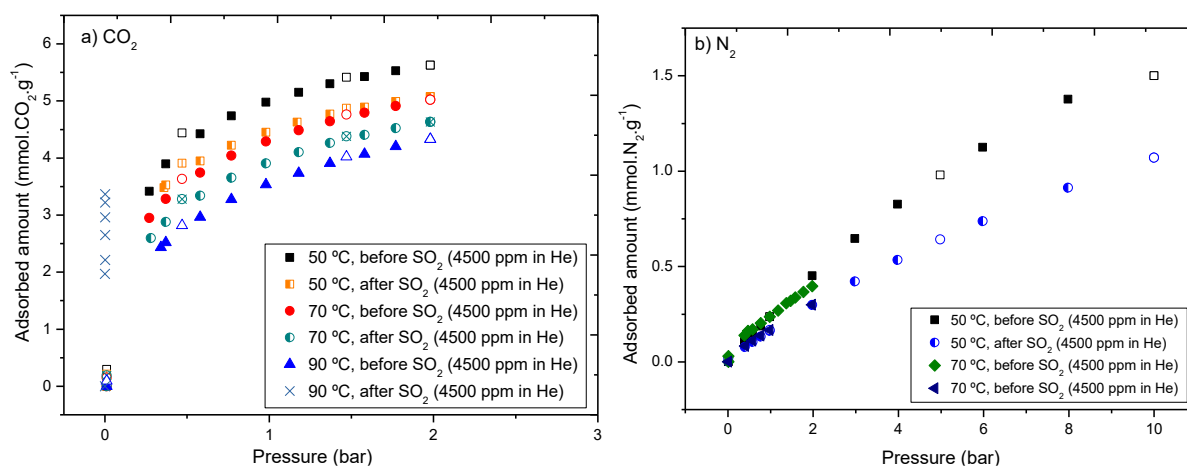
Source: by author (2024).

It is possible to observe in Figure 27 that for all scenarios studied, there was a reduction in the adsorption capacity of the 13XBF zeolite. However, it is worth highlighting the drastic behavior change observed in relation to N_2 adsorption, which presents a marked reduction when the zeolite was previously exposed to SO_2, even after being degassed under a vacuum (0.01 bar) at 300 °C for 12 hours.

The decrease in adsorptive capacity in N_2 is consistent with the findings of elemental analysis (CHNS) and X-ray excited photoelectron spectroscopy (XPS), as already mentioned, the formation of elemental sulfur can cause a reduction in pore size (or even block them completely) because this element is primarily deposited in the pore pairs, causing a decrease in the space available for N_2 molecules to enter the zeolite.

Such a relationship can be established to justify the behavior shown in Figure 27 because the adsorption of N_2 is sensitive to different pore sizes, as it is considered a probe molecule, which allows inferences about the porous structure of the material, based on the other experiments carried out in this study.

The understanding of this pattern of behavior is that adsorption capacity of this gas may depend on the size and distribution of the adsorbent pores.

In view of Figure 27, it is possible to understand the effect of the presence of SO_2 against the adsorptive/desorptive capacity of zeolite 13XBF at 50º C. To elucidate the impact of this contaminant (SO_2) in the gaseous stream, Figure 28 shows the impact on the capacity of CO_2 capture from 13XBF zeolite under the optics of different temperatures (relative to the same total pressures).

Figure 28 - Impact on the capacity of 13XBF zeolite: (a) CO_2 at 50 ºC, (b) CO_2 at 70 ºC, (c) N_2 at 50 ºC, (d) N_2 at 70 ºC. The filled points represent the fresh sample of 13XBF zeolite and the points marked with X symbolize the adsorptive capacity of the 13XBF zeolite after contact with SO_2 (4500 ppm in He) for 12 hours.
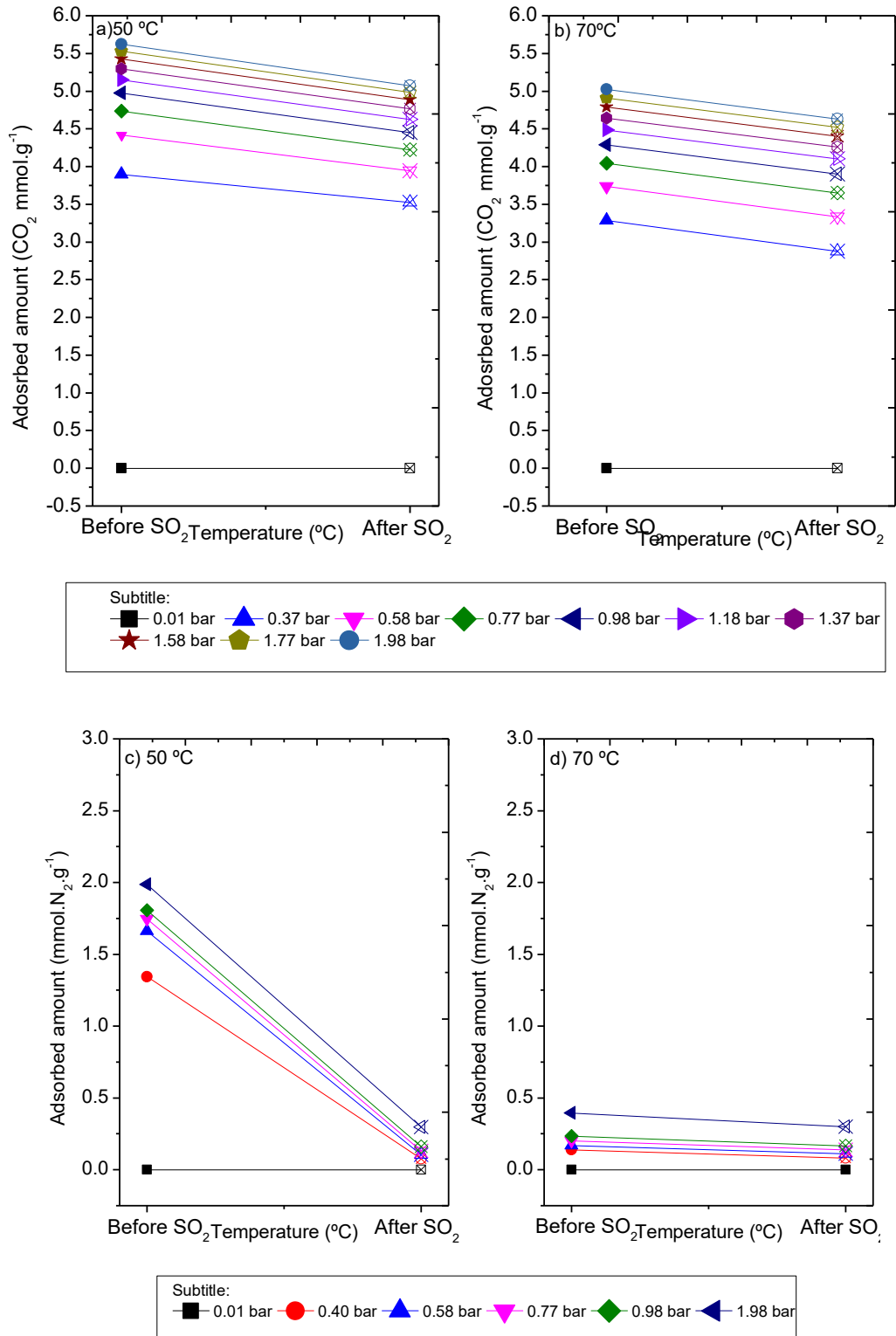
Source: by author (2024).

The data presented in Figure 28 demonstrate a significant reduction in the CO_2 and N_2 adsorption capacity when 13XBF zeolite is exposed to SO_2.

For carbon dioxide (CO_2), there is an average reduction of 10% in the adsorptive capacity of zeolite 13XBF for 50 ºC and 70 ºC in all pressure ranges studied. However, for N_2 this pattern of behavior is not observed: for 50 ºC there is a reduction of, on average, 91% for all pressure ranges presented, and, for 70 ºC, the decrease in the material's performance is approximately 32%.

This demonstrates that when the material is subjected to a stream of SO_2, even at low partial pressures (0.045 bar, 50 °C) for 12 hours, the adsorption becomes completely irreversible and even, after regenerating the material under typical degassing conditions for a zeolite (300 °C in vacuum for 12 hours), an amount of adsorbed SO_2 remains which causes a decrease in the amounts adsorbed at 50ºC.

Given the impact that sulfur dioxide has on the adsorptive capacity of zeolite 13XBF, variation in the isosteric heats of adsorption for CO_2 are presented before and after SO_2 contact (SO_2 diluted in He (4500 ppm)) for 12 hours at 50 and 70 ºC (Figure 29).

Figure 29 - Isosteric heat from CO_2 before and after contact with SO_2 (4500 ppm in He) at 50, 70, and 90 ºC for 12 hours
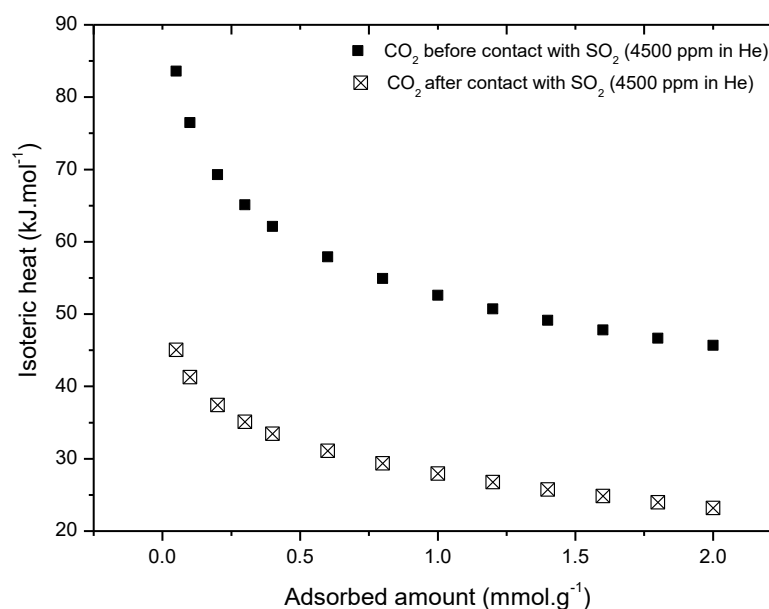
Source: by author (2024).

The reduction observed in the isosteric heats of adsorption of CO_2 presented in Figure 29 can be explained by the competition between SO_2 and CO_2 for the active sites of the zeolite, as this adsorbent has a high affinity for SO_2 (given the polarity of the molecule), which generates a greater interaction with the compensating cations of the zeolite than the quadrupole

moment of CO_2. It is observed, too, a reduction in the textural properties of the adsorbent after its exposure to a constant flow of SO_2 (4500 ppm in He). Such data (Figure 29) are consistent with the information presented in Table 9 and Figure 22 (b).

Therefore, it is necessary to analyze other data, such as Henry's constant. Table 12 presents a comparison between the Henry constants before and after SO_2 diluted in He (4500 ppm) contact for 12 hours at 50 and 70 ºC.

Table 13 - Summary of Henry's constant (K_h) from fresh sample of 13XBF zeolite *vs.* 13XBF zeolite after contact for 12 hours with SO_2 (4500 ppm in He)

	Temperature (ºC)	Fresh sample	After contact with SO_2^* for 12h	Reduction (%)
CO₂	50	27.063	23.947	11.51%
	70	20.811	16.573	20.36%
	90	13.392	8.644	35.45%
N₂	50	0.261	0.201	22.99%
	70	0.243	0.166	31.69%

Note(*): SO_2 diluted in He (4500 ppm).

Source: by author (2024).

The reduction in Henry's constant (Table 13) is consistent with the reduction in the textural properties of the 13XBF zeolite. As already mentioned, the sulfur adsorption process is irreversible (when the adsorbent is exposed to a constant flow of this contaminant for more than 12 hours) and this element is chemically adsorbed by the adsorbent, causing obstruction of the pores of this material, thus reflecting, in the reduction of Henry's constant. This observation is consistent with the findings of Yang et al. (2018) and Wijayanti et al., (2015).

Next, the effect of the contact time of SO_2 with the 13XBF zeolite in the CO_2/N_2 mixture (15/85 v/v) was evaluated, which are shown in

Figure 30 (a,c, and e) after 12 h of contact of the material with SO$_2$ (10 bar, 4500 ppm in He). Furthermore, in line with the research findings, the selectivity before and after contact with sulfur dioxide is also presented in

Figure 30 (b, d, and f).

Figure 30 – (a,c,e) CO_2/N_2 (15/85 v/v) binary adsorption/desorption isotherms for fresh zeolite (represented by black squares) and after SO2 contact for 12 hours (represented by red circles) at 50, 70 and 90 °C respectively and (b,d,f) the selectivity values estimated from Sips equation at 50, 70 and 90°C. Empty symbols represent the desorption points.
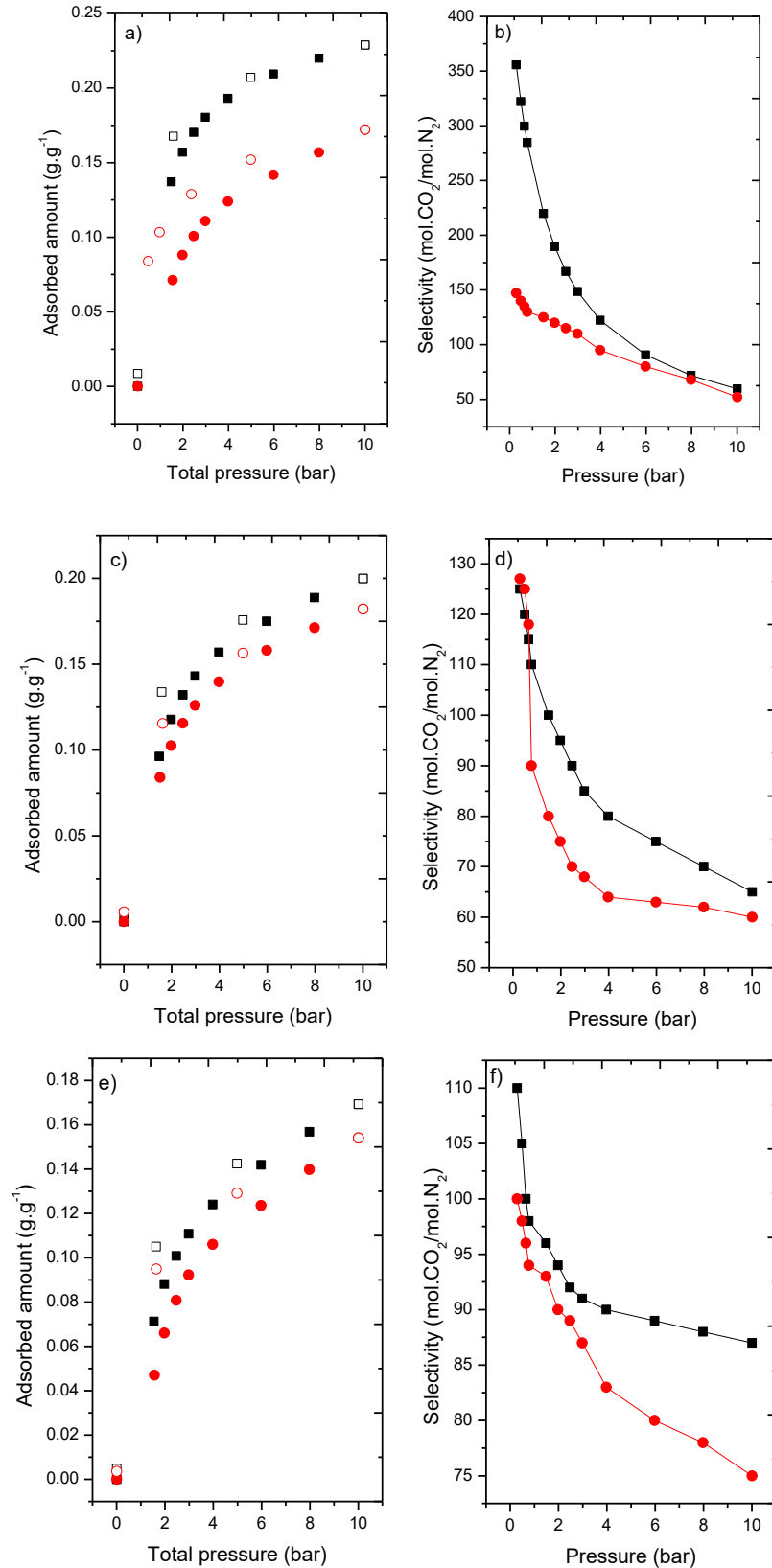
Source: by author (2024).

The binary CO_2/N_2 adsorption/desorption isotherms after 3 hours of contact of the adsorbent with SO_2 (10 bar, 4500 ppm in He) were not presented because, as already shown, until this exposure time the process is completely reversible, not presenting impact on the CO_2/N_2 multicomponent adsorption.

On the other hand, when the contact time is increased up to 12 h, the total amount adsorbed from the CO_2/N_2 mixture undergoes a reduction. It is important to highlight that, although there is a reduction in the total amounts adsorbed, the material follows the same pattern of behavior. This fact corroborates the hypothesis that sulfur is chemically adsorbed by 13XBF zeolite and alters the crystalline structure of the material resulting in the graphs shown in

Figure 30.

It is worth noting that the behavior exhibited by the material, when at 50 ºC, presents a hysteresis loop that is not observed for the fresh sample or for other temperatures.

This finding indicates that the bond between the adsorbent and the surface groups of the zeolite is stronger at a temperature of 50 ºC and what may have caused this difference in behavior is that the elementary S, originating from the SO_2 desorption process, tends to be desorbed from the surface of the material with increasing temperature.

Although temperatures of 70 and 90 ºC are not sufficient to completely desorb sulfur from the adsorbent, it is possible to observe that there is an influence on the behavior of the zeolite, which may be explained by the absence of hysteresis loops (

Figure 30 (c and e)).

This fact and the prolonged time of contact with SO_2 necessary to affect the textural properties of zeolite 13XBF leads to consider that the presence of SO_2 in low concentrations in the flue gas can be assumed in CCS project, as long as there is a low contact time between the gas stream and the adsorbent what if, in addition, the temperature of the gas entering the system is relatively high, such as TSA.

Furthermore, the temperature increases the effect of the SO_2 contact on CO_2 adsorption decreases, both in terms of total CO_2+N_2 adsorption capacity and CO_2/N_2 selectivity. That said, Figure 31 shows the selectivity as a function of the temperature of the virgin sample and after contact with SO_2 diluted in He (4500 ppm) for 12 hours.

Figure 31 - Selectivity as a function of temperature calculated from the Sips model
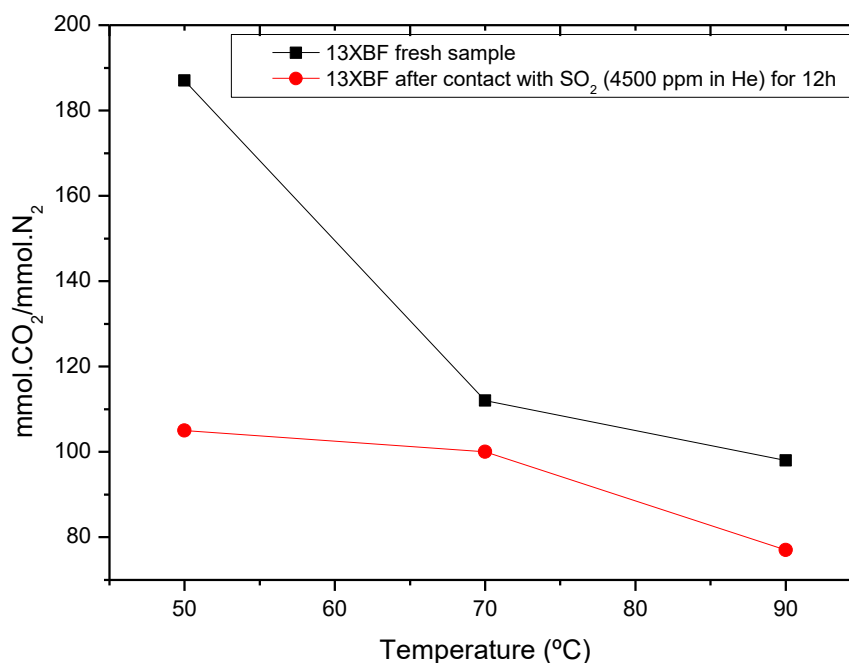
Source: by author (2024).

As can be seen in Figure 31, as the temperature increases, the difference between the CO_2/N_2 selectivity at 1 bar of the virgin sample and the sample after contact with SO_2 reduces. Supplying exhaust gases at a higher temperature reduces the effect of the presence of SO_2 on CO_2 capture and, even at 50 °C, the presence of this contaminant, despite considerably decreasing selectivity, zeolite 13XBF still maintains CO_2/N_2 selectivity considerably high as well as the CO_2 adsorption capacity.

Finally, having analyzed the effects of SO_2 (4500 ppm in He) on the 13XBF zeolite, we move on to evaluating the material when subjected to different adsorption/desorption cycles, as such information is crucial for the success of CCS systems, as the constant reuse of the

material is a crucial factor in the process, aiming to reduce the amount of solid waste produced in the capture of CO_2. Thus, in order to study whether the effect of SO_2 on CO_2 capture was cumulative or not, two research scenarios were outlined, which are presented in

Figure **32**.

Figure 32 - Experimental design to evaluate whether the effect of SO_2 on CO_2 capture is cumulative. The black line represents a single contact with diluted SO_2 (4500 ppm in He) for 12 hours and the red line represents successive contacts between CO_2 adsorption/desorption cycles with diluted SO_2 (4500 ppm in He) for 12 hours.
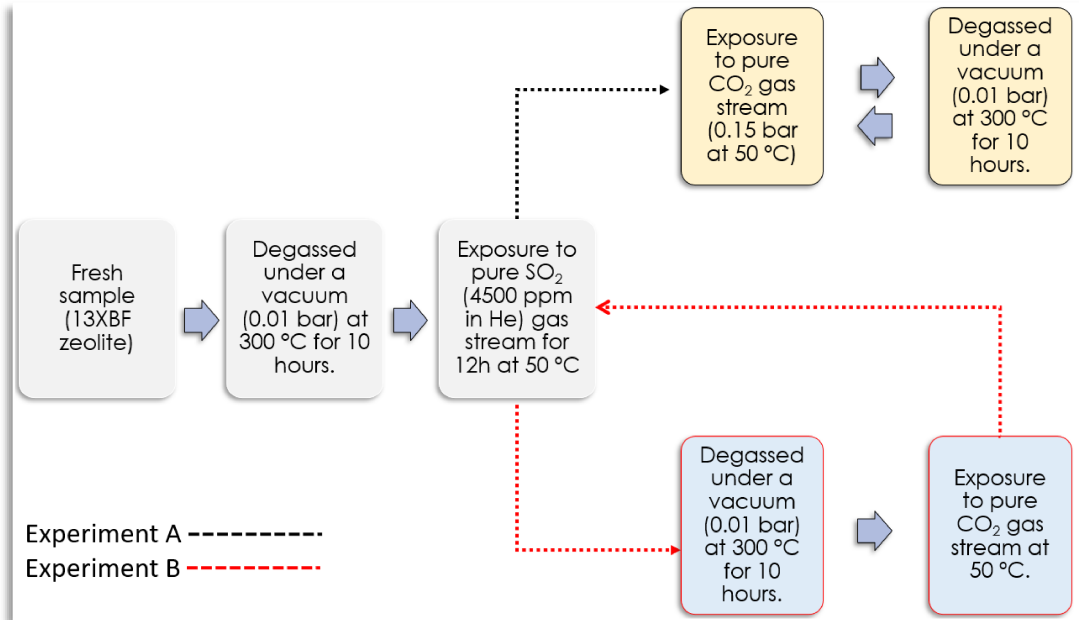
Source: by author (2024).

Based on the experimental design presented in

Figure 32, the data set shown in Figure 33 was generated, relating to experimental path A.

Figure 33 – (a) Evaluation of susceptible adsorption/desorption cycles: experimental path A. (b) Explanation of the loss of adsorption capacity of 13XBF zeolite after successive contact with SO2 (4500 ppm on He). Empty symbols represent the desorption points.
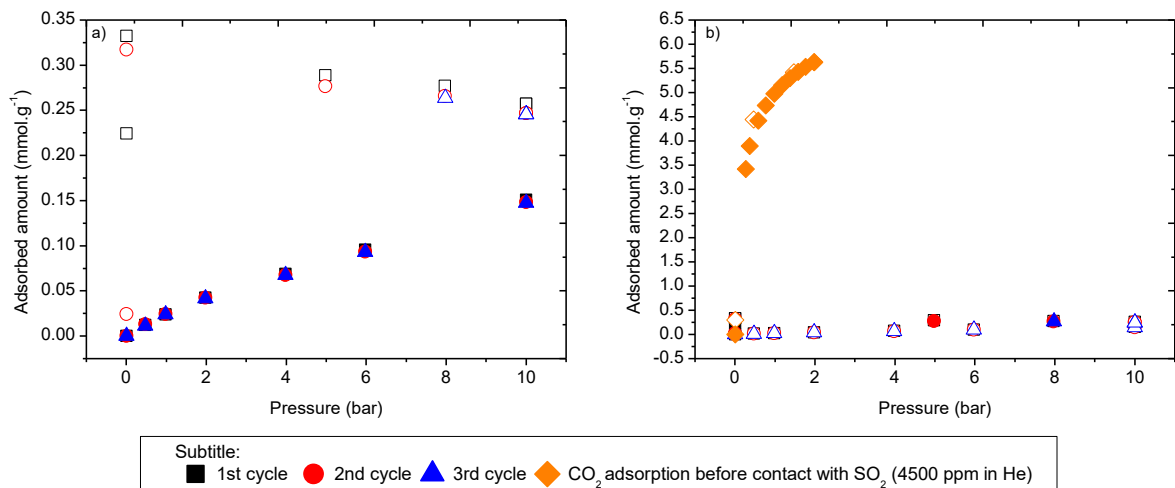
Source: by author (2024).

It can be seen in Figure 33 that, although the amount of CO_2 adsorption remains constant after contact with SO_2 (4500 ppm in He), as shown in Figure 33 (a), there is a significant loss in the adsorption capacity of the 13XBF zeolite when inserted into a constant flow of CO_2 under the same temperature and pressure conditions (Figure 33 (b)) although it is not possible to completely desorb the SO_2 present in the adsorbent.

This finding leads to the hypothesis that CCS systems may be able to withstand the presence of SO_2 in the gas stream, without the need for a gas pre-treatment unit. This observation translates into significant financial savings for projects of this nature.

To provide greater basis for the previous finding, we proceeded to experimental scenario B (shown in

Figure **32**), in which there was contact between the 13XBF zeolite, between CO_2 adsorption/desorption cycles, with SO_2 diluted in He (4500 ppm) for 12 hours, followed by degassed under a vacuum (0.01 bar) at 300 °C for 12 hours (Figure 34).

Figure 34 - Relationship between the amount of CO_2 adsorbed in each cycle and the amount of CO_2 adsorbed from the virgin sample. The blue dots refer to a single contact with diluted SO_2 (4500 ppm SO2 in He) for 12 hours between the 1st and 2nd cycle, while the orange dots refer to successive contacts between cycles with diluted SO_2. The amounts of CO_2 adsorbed in each cycle are at 50 °C and 0.15 bar.
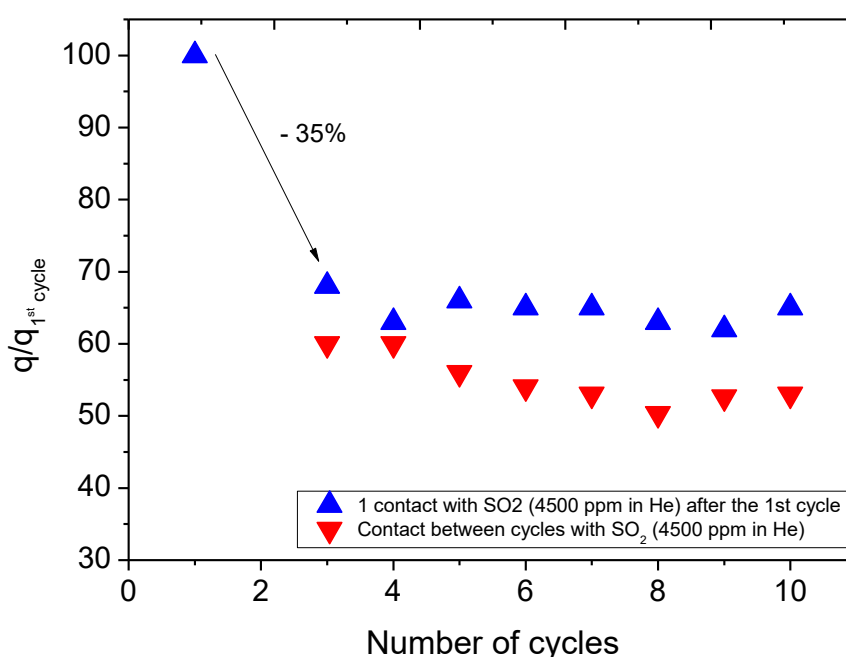
Source: by author (2024).

According to the data collected (Figure 34), it can be concluded that the effect of the presence of SO_2 on CO_2 capture is not cumulative. After the 1st contact, there is a drop in CO_2 adsorption capacity of approximately 35%. However, it was observed that with or without successive contacts with SO_2, the CO_2 adsorption capacity remained practically constant over the 10 cycles studied.

In order to study the regeneration of the adsorbent after contact with SO2, desorption tests were carried out on a magnetic suspension balance. Thus, four adsorbent regeneration configurations were evaluated:

    a. vacuum at 50°C for 12 hours,

    b. vacuum at 300°C for 12 hours

    c. under N_2 flow 50 mLmin^{-1} at 300 °C for 12 h

    d. under N_2 flow 50 mLmin^{-1} at 350 °C for 12 h

In each of these configurations for regeneration of the adsorbent, the regeneration capacity of the material was evaluated by gravimetry, that is, the ratio of the amount of SO_2 desorbed in relation to the amount adsorbed at a pressure of 0.045 bar, at 50 °C. The data obtained was summarized in Table 14.

Table 14 - Adsorbent regeneration tests after contact for 12 hours with diluted SO_2 (4500 ppm in He) at 50 °C.

Test	Temperature (°C)	Degassed conditions	(%) Regeneration
a.	50	vacuum	0
b.	300	vacuum	26
c.	300	N_2 50 mL.min^{-1}	27
d.	350	N_2 50 mL.min^{-1}	31

Source: by author (2024).

From Table 14 it can be seen that in no case was it possible to completely desorb the SO2 previously adsorbed on the zeolite surface. This finding was already expected and is consistent with the other findings of the present study, as there is evidence of sulfur chemisorption in the 13XBF zeolite, permanently altering its pore structure.

Furthermore, by increasing the temperature, part of the SO_2 can be desorbed, reaching just over 30% at 350 °C for 12 hours under inert gas flow. These results are consistent with the loss of capacity of the 13XBF zeolite when subjected to SO_2 flow, because, as seen previously, after contact the textural properties reduce by this order of magnitude and the amount of adsorbed CO_2 also drops by approximately 30%.

This fact and the prolonged time of contact with SO_2 necessary to affect the textural properties of zeolite 13XBF leads us to consider that the presence of SO_2 in low concentrations in the flue gas can be assumed in CCS project, as long as there is a low contact time between the gas stream and the adsorbent what if, in addition, the temperature of the gas entering the system is relatively high, such as TSA.

5 CONCLUSIONS

The present study assesses the impact of the presence of sulfur dioxide (SO_2) on CO_2 capture, under post-combustion scenario conditions using adsorption data (multi and single component) in 13X Binder Free (13XBF) zeolite, and application of mathematical models to describe the equilibrium conditions.

Among the gases released by biomass combustion, CO_2 and N_2 are the most abundant components, although humidity and SO_2 are always present in percentages that depend on the combustion methodology.

For this purpose, CO_2, N_2 and SO_2 adsorption/desorption equilibrium data (4500 ppm in He) of the pure and mixed components were obtained, under conditions of pressure, temperature, and concentration typical of those found in the post-combustion scenario. Furthermore, a mathematical model was applied to estimate the CO_2/N_2 and SO_2/CO_2 adsorption selectivity.

That said, it was concluded that:

a. The presence of sulfur dioxide (SO_2) in a gas stream has been found to significantly impact the adsorption capacity of zeolite for carbon dioxide (CO_2) and nitrogen (N_2). This effect is likely due to changes in the textural properties of the zeolite following prolonged exposure to SO_2. Observations revealed a notable reduction of approximately 35% in the total pore volume of the zeolite, indicating a diminished ability to adsorb CO_2 and N_2 molecules effectively.

b. Under the experimental conditions examined in this study, it was noted that thermodynamic equilibrium was not attained. This was evident as the quantity of sulfur dioxide (SO_2) adsorbed by 13XBF zeolite continued to rise in direct proportion to the duration of exposure to the gas stream. Consequently, it was observed that the adsorption process for SO_2 progresses at a notably slower rate compared to carbon dioxide (CO_2). This phenomenon aligns with findings in existing literature, suggesting that the sluggish adsorption of SO_2 can be attributed to diffusion control within the material's pores.

c. The adsorption of sulfur dioxide (SO_2) was found to be irreversible across all investigated temperatures (50, 70, and 90 ºC). However, an interesting observation was made regarding the reversibility of the adsorption process after 3 hours of contact at these temperatures, allowing for the recovery of the sample. It's important to note that this reversible phenomenon was not observed when the sample remained in contact with SO_2 for a prolonged duration of 12 hours.

d. The affinity difference relative to CO_2 and SO_2 molecules derives from molecule multipole moments and polarizability. SO_2 molecule has stronger affinity to the adsorbent but the more effective CO_2 packing releases higher heat of adsorption.

e. XPS analysis revealed that elemental sulfur (S) is formed when zeolite is exposed to a constant flow of SO_2. The formation of elemental sulfur limits the thermal regeneration, suggesting that chemisorption is one of the mechanisms of adsorption present.

f. The effect of the presence of SO_2 on CO_2 capture is not cumulative. After the 1st contact, there is a drop in CO_2 adsorption capacity of approximately 35%

In summary, it stands observed that the presence of SO_2 in low concentrations in the flue gas can be assumed in CCS project, as long as there is a low contact time between the gas stream and the adsorbent what if, in addition, the temperature of the gas entering the system is relatively high, such as TSA, since used 13XBF zeólita.

Finally, it is important to highlight that the presented results are important for important to feed future simulation models.

5.1 Suggestion for future work

As complementary suggestions for future work, it is proposed:

a. To analyze the effect of the joint action of water vapor, carbon monoxide (CO), and SO_2 on the CO_2 adsorption capacity of zeolite 13XBF.

b. Experimentally determine the maximum contact time of 13XBF zeolite with SO_2 so that the adsorption is reversible while seeking to understand the possible effects of deactivation of the adsorbent material;

c. Use molecular simulation tools to carry out a study at the molecular level to assess the competition between CO_2 and SO_2.

d. Evaluate the CO_2 adsorption capacity of zeolite 13XBF against a ternary mixture of $CO_2/H_2O/SO_2$.

REFERENCES

ARAKAWA, Kenji; MATSUDA, Satoshi; KINOSHITA, Hiroo. SOx poisoning mechanism of NOx selective reduction catalysts. **Applied Surface Science.** Japan, p. 382-386. 12 fev. 1997.

ARDILA, Yurany Camacho; FIGUEROA, Jaiver Efren Jaimes; LUNELLI, Betânia Hoss; MACIEL FILHO, Rubens; MACIEL, Maria Regina Wolf. **Syngas production from sugarcane bagasse in a circulating fluidized bed gasifier using Aspen Plus™**: modelling and simulation. Holanda, 2012. p. 1093-1097. DOI: 10.1016/B978-0-444-59520-1.50077-4.

BAGREEV, Andrey.; RAHMAN, Habibur.; BANDOSZ, Teresa. Thermal regeneration of a spent activated carbon previously used as hydrogen sulfide adsorbent. **Carbon**, Holanda. v. 39, n. 9, p. 1319–1326, ago. 2001. DOI: 10.1016/S0008-6223(00)00266-9.

BAHAMON, Daniel; VEGA, Lourdes. Systematic evaluation of materials for post-combustion CO_2 capture in a Temperature Swing Adsorption process. **Chemical Engineering** Journal, Estados Unidos da América, v. 284, p. 438–447, 15 jan. 2016. DOI: 10.1016/j.cej.2015.08.098.

BASTOS-NETO, Moisés; AZEVEDO, Diana Cristina Silva; LUCENA, Sebastião Mardônio Pereira. Assessing mass transfer rates in porous adsorbents using gas adsorption microcalorimetry. **Chemical Engineering Science**, Brazil, 2020. DOI: 10.1016/j.ces.2020.115983.

BERG, Frederik; PASEL, Chistoph, ECKARD, Tobias; BATHEN, Dieter. Temperature Swing Adsorption in Natural Gas Processing: A Concise Overview. **ChemBioEng Reviews**, Paris, v. 6, n. 3, p. 59 – 71. DOI: 10.1002/cben.201900005. 17 abr. 2023

BRASIL. **Projeto de Lei PL 290/2020**. Câmara dos Deputados. Brasil: https://www.camara.leg.br/proposicoesWeb/prop_mostrarintegra?codteor=1857740, 2020.

BRITISH PETROLEUM CO. **Statistical Review of World Energy** 2022. v. 71. 2022. Disponível em: https://www.bp.com/content/dam/bp/business-sites/en/global/corporate/pdfs/energy-economics/statistical-review/bp-stats-review-2022-full-report.pdf. Acesso em: 11 ago. 2022.

BRUNAUER, E.; EMMETT, P. H.; TELLER, E. Adsorption of Gases in Multimolecular Layers. **Journal of the Chemical Society**, Italian, v. 60, p. 309-319, fev. 1938.

BUI, M.; ADJIMAN, C.S.; BARDOW, A.; ANTHONY, E. J.; BOSTON, A.; BROWN, S.; FENNELL, P. S.; FUSS, S.; GALINDO, A.; HACKETTL. A.; HALLETT, J.P.; HERZOG, J. W.; JACKSON, G.; KEMPER, J.; KREVOR, S.; MAITLAND, G. C.; MATUSZEWSKI, M.; METCALFE, I. S.; PETIT, C.; PUXTY, G.; REIMER, J.; REINER, D. M.; RUBIN, E. S.; SCOTT, S. A.; SHAH, N.; SMIT. B.; JRUSLER, J. PM. M; WEBLEY,P.; WILCOX, J.; DOWELL, D. M. Carbon capture and storage (CCS): the way forward. **Energy & Environmental Science,** Portugal, [S.L.], v. 11, n. 5, p. 1062-1176, 2018. DOI: https://doi.org/10.1039/C7EE02342A.

CABRAL, R. P.; DOWELL, N. MAC. A novel methodological approach for achieving £/MWh cost reduction of CO_2 capture and storage (CCS) processes. **Applied Energy**, Argentina, v. 205, p. 529–539, 2017.

CARDOSO, Manuela Gomes. **Estudo da adsorção do íon amônio utilizando zeólitas naturais e sintetizadas a partir do rejeito do beneficiamento do carvão.** 2016. 132 f. Tese (Doutorado) - Curso de Programa de Pós-Graduação em Engenharia Química., Escola de Engenharia., Universidade Federal do Rio Grande do Sul, Porto Alegre, 2016. Disponível em: https://lume.ufrgs.br/handle/10183/147531. Acesso em: 14 jan. 2023.

CAVENATI, S.; GRANDE, C. A.; RODRIGUES, A. E. Adsorption Equilibrium of Methane, Carbon Dioxide, and Nitrogen on Zeolite 13X at High Pressures. **Journal of Chemical & Engineering Data**. Washington, v. 49, n. 4, p. 1095–1101, 1 jul. 2004.

CHEN, Rong; ZHANG, Tongsheng; GUO, Yiqun; WANG, Jiawei; WEI, Jiangxiong; YU, Qijun. Recent advances in simultaneous removal of SO2 and NOx from exhaust gases: removal process, mechanism and kinetics. **Chemical Engineering Journal**, Washington, v. 420, p. 127588, set. 2021. Elsevier BV. DOI: 10.1016/j.cej.2020.127588.

COLLS, Jeremy; TIWARY, Abhishek. **Air Pollution:** Measurement, Modelling and Mitigation. 3. ed. Londres, England: CRC Press, 2009.

COMISSÃO EUROPEIA. Comunicação da Comissão ao Parlamento Europeu, ao Conselho Europeu, Comitê Econômico e Social Europeu e ao Comitê das Regiões. **Pacto Ecológico Europeu.** Bruxelas, 2019. Disponível em: https://eur-lex.europa.eu/resource.html?uri=cellar:b828d165-1c22-11ea-8c 1f-01aa75ed71a1.0008.02/DOC_1&format=PDF. Acesso em: 15 fev. 2022.

CORMOS, Calin-Cristian. Oxy-combustion of coal, lignite and biomass: a techno-economic analysis for a large-scale carbon capture and storage (ccs) project in romania. **Fuel**, Germany, v. 169, p. 50-57, abr. 2016. Elsevier BV. DOI: http://dx.doi.org/10.1016/j.fuel.2015.12.005.

CUI, Yuanjing; YUE, Yanfeng; QIAN, Guodong; CHEN, Banglin. Luminescent Functional Metal–Organic Frameworks. **Chemical Reviews**, Italian, v. 112, n. 2, p. 1126-1162, 21 jun. 2011. American Chemical Society (ACS). http://dx.doi.org/10.1021/cr200101d.

DANCKWERTS, P. V. The reaction of CO with ethanolamines. **Chemical Engineering Science**, Washington, v. 34, n. 1, p. 443–446, 1979.

DANTAS, Tirzhá Lins Porto. **Separação de dióxido de carbono por adsorção a partir de misturas sintéticas do tipo gás de exaustão**. 2009. 172 f. Tese (Doutorado) - Curso de Curso de Programa de Pós-Graduação em Engenharia Química, Universidade Federal de Santa Catarina, Florianópolis, 2009. Disponível em: https://repositorio.ufsc.br/bitstream/handle/123456789/92549/262745.pdf?sequence=1&isAllowed=y. Acesso em: 14 jun. 2022.

DARDE, Victor; THOMSEN, Kaj; VAN WELL, Willy J.M.; STENBY, Erling Chilled ammonia process for CO_2 capture**.** Germany, v. 1, n. 1, p. 1035-1042, fev. 2009. Elsevier BV. http://dx.doi.org/10.1016/j.egypro.2009.01.137.

DENG, Hua; YI, Honghong; TANG, Xiaolong; YU, Qiongfen; NING, Ping; YANG, Liping. Adsorption equilibrium for sulfur dioxide, nitric oxide, carbon dioxide, nitrogen on 13X and 5A zeolites. **Chemical Engineering Journal,** Germany, v. 188, p. 77-85, abr. 2012. Elsevier BV. http://dx.doi.org/10.1016/j.cej.2012.02.026.

DO, D. D. Adsorption Analysis: Equilibria and Kinetics (With Cd Containing Computer Matlab Programs). Holand, **World Scientific**, v. 2, september 1998. DOI: https://doi.org/10.1142/p111.

DUTTA, Prabir K.; CARRADO, Kathleen A.; AUERBACH, Scott M**. Handbook of Zeolite Science and Technology.** New York: Marcel Dekker, Inc, 2003.

ENZWEILER, Heveline; COUTINHO, Elisa Barbosa; SCHWAAB, Marcio. Cinzas de casca de arroz como fonte alternativa de silício para a síntese de zeólita beta. **Revista Eletrônica em Gestão, Educação e Tecnologia Ambiental**. Santa Catarina, v. 17, n. 17, p. 3284-3292, 2014. DOI: http://dx.doi.org/10.5902/2236117010478.

FIGUEROA, Jaiver Efren Jaimes; ARDILA, Yurany Camacho; LUNELLI, Betania H.; MACIEL FILHO, Rubens; MACIEL, Maria Regina Wolf. Evaluation of pyrolysis and steam gasification processes of sugarcane bagasse in a fixed bed reactor. **Chemical Engineering Transactions**, Milan, v. 11, p. 171-180, dez. 2013. AIDIC: Italian Association of Chemical Engineering. DOI: http://dx.doi.org/10.3303/ACOS1311018.

FIGUEROA, José D.; FOUT, Timothy; PLASYNSKI, Sean; MCILVRIED, Howard; SRIVASTAVA, Rameshwar D. Advances in CO_2 capture technology—The U.S. Department of Energy's Carbon Sequestration Program. **International Journal Of Greenhouse Gas Control**, Washington, v. 2, n. 1, p. 9-20, jan. 2008. Elsevier BV. http://dx.doi.org/10.1016/s1750-5836(07)00094-1.

FRIBERG, I.; SADOKHINA, N.; OLSSON, L. The effect of Si/Al ratio of zeolite supported Pd for complete CH4 oxidation in the presence of water vapor and SO2. **Applied Catalysis B: Environmental,** Barcelona, v. 250, p. 117–131.

GOMES, Diego Angelo de Araújo. **Adsorção de n-parafinas na faixa de c10 a c13 sobre materiais microporosos. 2014**. 114 f. Tese (Doutorado) - Curso de Curso de Programa de Pós-Graduação em Engenharia Química, Escola Politécnica, Universidade Federal da Bahia, Salvador, 2014. Disponível em: https://repositorio.ufba.br/bitstream/ri/18862/1/TESE%20DE%20DOUTORADO_Diego_Gomes.pdf. Acesso em: 25 nov. 2022.

GUIMARÃES JÚNIOR, Walber Gonçalves. **Estudo Teórico da Adsorção de Gases Leves nas Redes Metalorgânicas SIFSIX-2-Cu, SIFSIX-2-Cu-i e SIFSIX-3-Cu**. 2017. 95 f. Dissertação (Mestrado) - Curso de Química, Universidade Federal de Itajubá, Itajubá, 2017. Disponível em: https://repositorio.unifei.edu.br/xmlui/bitstream/handle/123456789/807/dissertacao_guimaraes_junior_2017.pdf?sequence=1&isAllowed=y. Acesso em: 14 jan. 2022.

GUTIERREZ-ORTEGA, A.; MONTES-MORÁN, M.A.; PARRA, J.B.; SEMPERE, J.; NOMEN, R.; GONZALEZ-OLMOS, R.. Comparative study of binderless zeolites and carbon molecular sieves as adsorbents for CO_2 capture processes. **Journal Of CO_2 Utilization**, Huston, v. 61, p. 102012, jul. 2022. Elsevier BV. DOI: http://dx.doi.org/10.1016/j.jcou.2022.102012.

H. PAN; J.A. RITTER; P.B. BALBUENA. Isosteric Heat. *Em*: **Functional Theory**. 1. ed. Noruega, s. n., v. 1159–1166p. 1159–1166.

HARLICK, P. J. E.; TEZEL, F. H. An experimental adsorbent screening study for CO2 removal from N2. **Microporous and Mesoporous Materials**, Bruxelas, v. 76, n. 1–3, p. 71–79, 2004.

INTERNATIONAL ENERGY AGENCY (org). **Global Energy Review 2021b**: assessing the effects of economic recoveries on global energy demand and co2 emissions in 2021. Holanda: International Energy Agency, 2021.

INTERNATIONAL ENERGY AGENCY (org.). **Net Zero by 2050**: a roadmap for the global energy sector. France: International Energy Agency, 2021a. Disponível em: www.iea.org/t&c/. Acesso em: 05 jan. 2023.

JIA, Xicheng; KHAN, Wasim; WU, Zhijie; CHOI, Jungkyu; YIP, Alex C.K.. Modern synthesis strategies for hierarchical zeolites: bottom-up versus top-down strategies. **Advanced Powder Technology,** Japan, v. 30, n. 3, p. 467-484, mar. 2019. Elsevier BV. DOI: http://dx.doi.org/10.1016/j.apt.2018.12.014

JOOS, Lennart; SWISHER, Joseph A.; SMIT, Berend. Molecular Simulation Study of the Competitive Adsorption of H2O and CO2 in Zeolite 13X. **Langmuir,** Washington, v. 29, n. 51, p. 15936-15942, 12 dez. 2013. American Chemical Society (ACS). DOI: http://dx.doi.org/10.1021/la403824g.

KIM, Kyung-Min; OH, Hyun-Taek; LIM, Seung-Jun; HO, Keon; PARK, Yongha; LEE, Chang-Ha. Adsorption Equilibria of Water Vapor on Zeolite 3A, Zeolite 13X, and Dealuminated Y Zeolite. **Journal Of Chemical & Engineering Data**, Washington, v. 61, n. 4, p. 1547-1554, 11 mar. 2016. American Chemical Society (ACS). DOI: http://dx.doi.org/10.1021/acs.jced.5b00927.

KORALEGEDARA, N. H.; PINTO, Patricio X. DIONYSIOU, Dionysios D.; AL-ABED, Souhail R.. Recent advances in flue gas desulfurization gypsum processes and applications – A review. **Journal of environmental management**, Noruega, v. 251, n. 109572, p. 109572, 2019. DOI: 10.1016/j.jenvman.2019.109572

KUMAR, Santosh; SRIVASTAVA, Rohit; KOH, Joonseok. Utilization of zeolites as CO2 capturing agents: advances and future perspectives. **Journal Of Co2 Utilization**, Germany, v. 41, p. 101251, out. 2020. Elsevier BV. DOI: http://dx.doi.org/10.1016/j.jcou.2020.101251.

LEE, Jong-Seok; KIM, Jong-Hwa; KIM, Jin-Tae; SUH, Jeong-Kwon; LEE, Jung-Min; LEE, Chang-Ha. Adsorption Equilibria of CO2 on Zeolite 13X and Zeolite X/Activated Carbon Composite. **Journal Of Chemical & Engineering Data**, Japan, v. 47, n. 5, p. 1237-1242, 26 jun. 2002. American Chemical Society (ACS). DOI: http://dx.doi.org/10.1021/je020050e.

LI, Gang; XIAO, Penny; WEBLEY, Paul A.; ZHANG, Jun; SINGH, Ranjeet. Competition of CO2/H2O in adsorption based CO2 capture. **Energy Procedia**, China, v. 1, n. 1, p. 1123-1130, fev. 2009. Elsevier BV. DOI: http://dx.doi.org/10.1016/j.egypro.2009.01.148.

LI, Qingchun; XU, Wenjun; LIANG, Xin; LIU, Baogen; WU, Qingding; ZENG, Zheng; LI, Liqing; MA, Xiancheng. Specific alkali metal sites as CO2 traps in activated carbon with different pore size for CO2 selective adsorption: gcmc and dft simulations. **Fuel**, China, v. 325, p. 124871, out. 2022. Elsevier BV. DOI: http://dx.doi.org/10.1016/j.fuel.2022.124871.

MATEUS, Sérgio Filipe Cardoso. **Simulação de Curvas de Ruptura em Leito Fixo com Dimensionamento de Válvulas**. 2009. 112 f. Tese (Doutorado) - Curso de Curso de

Programa de Pós-Graduação em Química, Departamento de Química, Universidade de Aveiro, Aveiro, 2009. Disponível em: https://ria.ua.pt/bitstream/10773/3122/1/2010000309.pdf. Acesso em: 9 jan. 2023.

MENDES, Kristopher Gums Xavier. **Estudos da reatividade de coques de carvões catarinenses através da gaseificação com CO_2**. 1995. 92 f. Tese (Doutorado) - Curso de Curso de Programa de Pós-Graduação em Engenharia Química, Centro Tecnológico, Universidade Federal de Santa Catarina, Florianópolis, 1995. Disponível em: https://repositorio.ufsc.br/xmlui/bitstream/handle/123456789/157958/101457.pdf?sequence=1&isAllowed=y. Acesso em: 7 set. 2022.

MENG, Yuan; JU, Tongyao; HAN, Siyu; GAO, Yuchen; LIU, Jiwei; JIANG, Jianguo. Exploring the stability on exposure to acid impurities of polyethyleneimine-functionalized silica for post-combustion CO_2 capture**. Chemical Engineering Journal**, Tokyo, v. 421, p. 127754, out. 2021. Elsevier BV. DOI: http://dx.doi.org/10.1016/j.cej.2020.127754.

MEREL, Jérôme; CLAUSSE, Marc; MEUNIER, Francis. Experimental Investigation on CO2 Post−Combustion Capture by Indirect Thermal Swing Adsorption Using 13X and 5A Zeolites. Industrial & Engineering Chemistry Research, Washington, v. 47, n. 1, p. 209-215, 11 dez. 2007. **American Chemical Society (ACS)**. DOI: http://dx.doi.org/10.1021/ie071012x.

MIANO, F. Adsorption of hydrocarbon vapour mixtures onto zeolite 5A**. Colloids And Surfaces A:** Physicochemical and Engineering Aspects, [S.L.], v. 110, n. 1, p. 95-104, maio 1996. Elsevier BV. DOI: http://dx.doi.org/10.1016/0927-7757(95)03439-0.

MOFARAHI, M.; GHOLIPOUR, F. Gas adsorption separation of CO2/CH4 system using zeolite 5A**. Microporous and Mesoporous Materials**, Chile, v. 200, p. 1–10, dez. 2014.

MORALES-OSPINO, Rafael Augusto. **CO_2 post-combustion capture from a coal-fired power plant: assessment of commercial and synthesized zeolites and moving bed simulations.** 2021. 133 f. Tese (Doutorado) - Curso de Programa de Pós-Graduação em Engenharia Química, Centro de Tecnologia, Universidade Federal do Ceará, Fortaleza, 2021. Disponível em: https://repositorio.ufc.br/bitstream/riufc/61232/1/2021_tese_ramospino.pdf. Acesso em: 30 set. 2022.

MORALES-OSPINO, Rafael; SANTIAGO, Rafaelle Gomes; SIQUEIRA, Rafael Magalhães; AZEVEDO, Diana Cristina Silva de; BASTOS-NETO, Moises. Assessment of CO2 desorption from 13X zeolite for a prospective TSA process. **Adsorption**, [S.L.], v. 26, n. 5, p. 813-824, 14 dez. 2019. Springer Science and Business Media LLC. DOI: http://dx.doi.org/10.1007/s10450-019-00192-5.

MORALES-OSPINO, Rafael; SANTOS, Vitória N.; LIMA, Antônio R. A.; TORRES, A. Eurico B.; VILARRASA-GARCÍA, Enrique; BASTOS-NETO, Moises; CAVALCANTE, Celio L.; AZEVEDO, Diana C. S.; MARQUES, Carolina R. M.; AQUINO, Thiago F. de. Parametric Analysis of a Moving Bed Temperature Swing Adsorption (MBTSA) Process for Postcombustion CO2 Capture. **Industrial & Engineering Chemistry Research**, Brazil, v. 60, n. 29, p. 10736-10752, 27 abr. 2021. American Chemical Society (ACS). DOI: http://dx.doi.org/10.1021/acs.iecr.0c05067.

MOREIRA, Davi Diego da Silva. **Influência do SO_2 na captura do CO_2 em condições de pós-combustão.** 2022. 97 f. Dissertação (Mestrado) - Curso de Programa de Pós-Graduação em Engenharia Química, Centro de Tecnologia, Universidade Federal do Ceará, Fortaleza,

2022. Disponível em:
https://repositorio.ufc.br/bitstream/riufc/69462/1/2022_dis_ddsmoreira.pdf. Acesso em: 25 set. 2022.

MURALI, R. Surya; SANKARSHANA, T.; SRIDHAR, S.. Air Separation by Polymer-based Membrane Technology. **Separation & Purification Reviews**, Colombia, v. 42, n. 2, p. 130-186, jan. 2013. Informa UK Limited. DOI: http://dx.doi.org/10.1080/15422119.2012.686000.

NASCIMENTO, R. **Adsorção**: aspectos teóricos e aplicações ambientais. 1. ed. Fortaleza: Imprensa Universitária, 2014.

NETO, S.; SZKLO, A.; ROCHEDO, P. R. R. Calcium looping post-combustion CO_2 capture in sugarcane bagasse fuelled power plants. **International Journal of Greenhouse Gas Control**, Estocolmo, v. 110, 2021.

NICODÈME, Thibault; BERCHEM, Thomas; JACQUET, Nicolas; RICHEL, Aurore. Thermochemical conversion of sugar industry by-products to biofuels. **Renewable And Sustainable Energy Review**s, Washington, v. 88, p. 151-159, maio 2018. Elsevier BV. DOI: http://dx.doi.org/10.1016/j.rser.2018.02.037

OJEDA-LÓPEZ, Reyna; VILARRASA-GARCÍA, Enrique; AZEVEDO, Diana C. S.; FELIPE, Carlos; CECILIA, Juan A.; RODRÍGUEZ-CASTELLÓN, Enrique. CO2 selectivity in CO2: ch4 and co2. **Fuel**, Washington, v. 324, p. 124242, set. 2022. Elsevier BV. DOI: http://dx.doi.org/10.1016/j.fuel.2022.124242.

OLIVEIRA, J. C. A. DE *et al.* Representative Pores: An Efficient Method to Characterize Activated Carbons. **Frontiers in Chemistry**, Viena, v. 8, 28 jan. 2021.

OSPINO, Rafael Augusto Morales. **Assessment of temperature swing adsorption configurations for CO₂ capture on zeolite** 13X. 2018. 100 f. Tese (Doutorado) - Curso de Curso de Programa de Pós-Graduação em Engenharia Química, Centro de Tecnologia, Universidade Federal do Ceará, Fortaleza, 2018. Disponível em: https://repositorio.ufc.br/bitstream/riufc/31578/7/2018_dis_ramospino.pdf. Acesso em: 03 jan. 2023.

OXFORD INSTITUTE FOR ENERGY STUDIES (org.). **Carbon capture, utilization and storage (CCUS):** barriers, enabling frameworks and prospects for climate change mitigation. OXFORD ENERGY FORUM, Oxford, v. 1, n. 130, p. 1–72, 2022.

PERA-TITUS, M. Porous inorganic membranes for CO2 capture: Present and prospects. **Chemical Reviews**, Londres, 22 jan. 2014.

POLANYI, M. The Potential Theory of Adsorption. **Science**, Germany, v. 141, n. 3585, p. 1010–1013, 13 set. 1963.

RACKLEY, S. A. Overview of carbon capture and storage. *Em*: **Carbon Capture and Storage**. Suécia, 2017. p. 23–36.

ROUQUEROL, F. Adsorption by Powders and Porous Solids Principles, Methodology and Applications. **Oxford**: Academic Press, Londres, 2014. v. 1. ed. 2.

RUFFORD, T.e.; SMART, S.; WATSON, G.C.y.; GRAHAM, B.F.; BOXALL, J.; COSTA, J.C. Diniz da; MAY, E.F.. The removal of CO2 and N2 from natural gas: a review of

conventional and emerging process technologies. **Journal Of Petroleum Science And Engineering**, Washingto, v. 94-95, p. 123-154, set. 2012. Elsevier BV. DOI: http://dx.doi.org/10.1016/j.petrol.2012.06.016.

RUTHVEN, D. **Principles of Adsorption and Adsorption Processes**. 1. ed. New York, Library of Congress Cataloging, 1984. v. 1.

SAMANTA, Arunkumar; ZHAO, An; SHIMIZU, George K. H.; SARKAR, Partha; GUPTA, Rajender. Post-Combustion CO2 Capture Using Solid Sorbents: a review. Industrial & Engineering Chemistry Research, Washington, v. 51, n. 4, p. 1438-1463, 21 nov. 2011. **American Chemical Society (ACS**). DOI: http://dx.doi.org/10.1021/ie200686q

SAYARI, A.; BELMABKHOUT, Y.; SERNA-GUERRERO, R. Flue gas treatment via CO2 adsorption. **Chemical Engineering Journal**, Texas, v. 171, n. 3, p. 760–774, jul. 2011.

SHABBANI, Hind Jihad Kadhim. **Determination and Validation of High-Pressure Equilibrium Adsorption Isotherms via a Volumetric System**. 2013. 58 f. Dissertação (Mestrado) - Curso de Chemical Engineering, Al-Qadisiya University, Tokyo, 2013.

SHAW, R.; MUKHERJEE, S. The development of carbon capture and storage (CCS) in India: A critical review. **Carbon Capture Science & Technology**, India, v. 2, mar. 2022.

SHI, Lei; YANG, Ke; ZHAO, Qiaopo; WANG, Haiyan; CUI, Qun. Characterization and Mechanisms of H2S and SO2 Adsorption by Activated Carbon. **Energy & Fuels**, Washington, v. 29, n. 10, p. 6678-6685, 5 out. 2015. American Chemical Society (ACS). DOI: http://dx.doi.org/10.1021/acs.energyfuels.5b0169

SIGOT, L.; DUCOM, G.; GERMAIN, P. Adsorption of hydrogen sulfide (H2S) on zeolite (Z): Retention mechanism. **Chemical Engineering Journal**, Texas, v. 287, p. 47–53, mar. 2016.

SIPS, R. On the structure of a catalyst surface. II. **The Journal of Chemical Physics**, Germany, v. 18, n. 8, p. 1024–1026, 1950.

SMIT, B.; MAESEN, T. L. M. Towards a molecular understanding of shape selectivity. **Nature**, Reino Unido, v. 451, n. 7179, p. 671–678, fev. 2008.

SOKOLAR, R.; NGUYEN, M. A Novel Process for the Containment of SO2 Emissions from Class C Fly Ash in the Fired Materials by Haüyne Formation. **Materials**, Colombia, v. 15, n. 19, p. 6701, 27 set. 2022.

SONG, Chunfeng; LIU, Qingling; JI, Na; DENG, Shuai; ZHAO, Jun; LI, Yang; SONG, Yingjin; LI, Hailong. Alternative pathways for efficient CO2 capture by hybrid processes—A review. **Renewable And Sustainable Energy Reviews,** Washington, v. 82, p. 215-231, fev. 2018. Elsevier BV. DOI: http://dx.doi.org/10.1016/j.rser.2017.09.040.

SRIVASTAVA, R. K.; JOZEWICZ, W. Flue gas desulfurization: the state of the art. **Journal of the Air & Waste Management Association** (2001), Paris, v. 51, n. 12, p. 1676–1688, 2001.

SUN, Y.; ZWOLIŃSKA, E.; CHMIELEWSKI, A. G. **Abatement technologies for high concentrations of NOx and SO2 removal from exhaust gases:** A review. Critical Reviews in Environmental Science and Technology, India, v. 46, n. 2, p. 119–142, 17 jan. 2016.

SWESTY, F. D. Thermodynamically Consistent Interpolation for Equation of State Tables. **Journal of Computational Physics,** Zurique, v. 127, n. 1, p. 118–127, ago. 1996.

THOMMES, Matthias; KANEKO, Katsumi; NEIMARK, Alexander V.; OLIVIER, James P.; RODRIGUEZ-REINOSO, Francisco; ROUQUEROL, Jean; SING, Kenneth S.W. Physisorption of gases, with special reference to the evaluation of surface area and pore size distribution (IUPAC Technical Report). **Pure And Applied Chemistry**, Zurique, v. 87, n. 9-10, p. 1051-1069, 2 jul. 2015. Walter de Gruyter GmbH. DOI: http://dx.doi.org/10.1515/pac-2014-1117.

TOTH, J. **State Equations of the Soilid-gas Ibterface Layers**. Acta chimical Academiae Scientiarum Hungaricae, Hungria, v. 69, p. 311–328, 1971.

TRIEBE, R. W.; TEZEL, F. H. Adsorption of nitrogen, carbon monoxide, carbon dioxide and nitric oxide on molecular sieves. **Gas Separation & Purification**, Argentina, v. 9, n. 4, p. 223–230, dez. 1995.

UGUINA, M.A.; SERRANO, D.P.; VAN GRIEKEN, R.; VÈNES, S. Adsorption, acid and catalytic changes induced in ZSM-5 by coking with different hydrocarbons. **Applied Catalysis A:** General, Argentina, v. 99, n. 2, p. 97-113, jun. 1993. Elsevier BV. DOI: http://dx.doi.org/10.1016/0926-860x(93)80093-6.

UNITED NATIONS. **Paris agreement.** Paris: 1998.

UNITED STATES. ENVIRONMENTAL PROTECTION AGENCY. (org.). **Sulfur Dioxide (SO$_2$) Pollution.** Disponível em: https://epa.gov/so2-pollution/setting-and-. Acesso em: 07 jan. 2024.

UNUABONAH, E. I.; OMOROGIE, M. O.; OLADOJA, N. A. Modeling in Adsorption: Fundamentals and Applications. **Composite Nanoadsorbents**. [s.l.] Elsevier, 2019. p. 85–118.

WALTON, K. S.; ABNEY, M. B.; DOUGLAS LEVAN, M. CO2 adsorption in Y and X zeolites modified by alkali metal cation exchange. **Microporous and Mesoporous Materials**, Portugal, v. 91, n. 1–3, p. 78–84, abr. 2006.

WIJAYANTI, Kurnia; ANDONOVA, Stanislava; KUMAR, Ashok; LI, Junhui; KAMASAMUDRAM, Krishna; CURRIER, Neal W.; YEZERETS, Aleksey; OLSSON, Louise. Impact of sulfur oxide on NH3-SCR over Cu-SAPO-34. **Applied Catalysis B**: Environmental, Barcelona, v. 166-167, p. 568-579, maio 2015. Elsevier BV. DOI: http://dx.doi.org/10.1016/j.apcatb.2014.11.043.

WOLFE, R.; SAMS, J. R. The Virial Theory of Adsorption and the Surface Areas of Solids. **The Journal of Physical Chemistry**, Oxford v. 69, n. 4, p. 1129–1135, 1 abr. 1965.

WORCH, Eckhard. Adsorption Technology in Water Treatment**. Fundamentals, Processes, And Modeling**, Espanha, 15 abr. 2021. De Gruyter. DOI:http://dx.doi.org/10.1515/9783110715507.

YANG, Guangpeng; DU, Xuesen; RAN, Jingyu; WANG, Xiangmin; CHEN, Yanrong; ZHANG, Li. Understanding SO2 Poisoning over Different Copper Species of Cu-SAPO-34 Catalyst: a periodic dft study. **The Journal Of Physical Chemistry** C, Oxford, v. 122, n. 37,

p. 21468-21477, 28 ago. 2018. American Chemical Society (ACS). DOI:
http://dx.doi.org/10.1021/acs.jpcc.8b06765.

YANG, Ralph T; QIAN, Kangyi; BUZANOWSKI, Mark A. Air-prepuri"cation by pressure
swing adsorption using single/layered beds**. Chemical Engineering Science,** Brazil. 2001.

YONG, Z; MATA, V; Rodrigues. Adsorption of carbon dioxide at high temperature—a
review**. Separation And Purification Technology,** Japan, v. 26, n. 2-3, p. 195-205, 1 mar.
2002. Elsevier BV. DOI: http://dx.doi.org/10.1016/s1383-5866(01)00165-4.

YU, C.-H.; HUANG, C.-H.; TAN, C.-S. A Review of CO2 Capture by Absorption and
Adsorption. **Aerosol and Air Quality Research,** China v. 12, n. 5, p. 745–769, 2012.

YUAN, Z.; EDEN, M. R.; GANI, R. Toward the Development and Deployment of Large-
Scale Carbon Dioxide Capture and Conversion Processes**. Industrial & Engineering
Chemistry Research**, China, v. 55, n. 12, p. 3383–3419, 30 mar. 2016.